

CORE-COLLAPSE SUPERNOVAE AND HOST GALAXY STELLAR POPULATIONS

PATRICK L. KELLY^{1,2} AND ROBERT P. KIRSHNER³*Draft version February 25, 2019*

ABSTRACT

We have used images and spectra of the Sloan Digital Sky Survey to examine the host galaxies of 519 nearby supernovae. The colors at the sites of the explosions, as well as chemical abundances, and specific star formation rates of the host galaxies provide circumstantial evidence on the origin of each supernova type. We examine separately SN II, SN IIn, SN I Ib, SN Ib, SN Ic, and SN Ic with broad lines (SN Ic-BL). The host galaxies of SN Ic, which explode at small host offsets, have exceptionally strongly star-forming, metal-rich, and dusty stellar populations near their centers. The SN Ic-BL and SN I Ib explode in exceptionally blue locations, and we find that their host galaxies have lower oxygen abundance than the hosts of their respective close spectroscopic cousins, SN Ic and SN Ib. The host galaxies of SN Ic-BL also exhibit strong central specific star formation rates. In contrast, we find no strong evidence for different environments for SN IIn compared to the sites of SN II. We take account of the source of the supernova discoveries, whether from targeted searches or from galaxy-impartial surveys, and show that these results are robust.

Subject headings: supernovae: general — stars: abundances — galaxies: star formation — gamma rays: bursts

1. INTRODUCTION

The only SN found in passive, elliptical galaxies are Type Ia (van den Bergh & Tammann 1991). Finding these events in galaxies without ongoing star formation is strong evidence that long-lived progenitors contribute to the observed SN Ia population. SN of other spectroscopic types have been discovered only in star-forming galaxies: that is why we think these SN types are explosions of massive, short-lived stars. Our aim here is to use more detailed information on the hosts to help sort out the origin of the varieties of core-collapse events. Host galaxy measurements have started to identify patterns among the environments of the many spectroscopic types of core-collapse supernovae (e.g., van Dyk et al. 1996; Modjaz et al. 2008; Kelly et al. 2008). Here, we construct a nearby sample of supernova hosts where ground-based images provide useful spatial resolution: for the median redshift in our sample ($z \sim 0.02$), one arcsecond corresponds to 400 parsecs⁵. We use images from SDSS Data Release 8 (DR 8) to measure the color at the supernova sites and to estimate the hosts' stellar masses, and Sloan spectra to determine the hosts' oxygen abundances, specific star formation rate (SFR), and the interstellar reddening. Although these are blunt tools for determining how star formation, stellar evolution, mass loss, and progenitor chemistry produce the diversity of core-collapse phenomena, circumstantial evidence can provide useful clues to these complex processes.

The primary SN spectroscopic classes are organized

around evidence of hydrogen and helium features (see Filippenko 1997 for a review). Young, massive stars with an intact hydrogen envelope at the time of their explosion yield hydrogen-rich spectra, the Type II class. When massive SN progenitors lose their hydrogen-rich shells, the core collapse and subsequent explosions can produce a variety of spectroscopic outcomes. SN Ib have a hydrogen-deficient spectrum that shows helium features, while SN Ic do not show either hydrogen or helium lines. The chameleon SN I Ib class shows the hydrogen lines of a SN II at first, but then shows helium lines, suggesting there is only a thin layer of hydrogen on the surface. Line widths are also important. The spectra of SN Ic sometimes show very broad lines, suggesting expansion of the surface at 0.1c: these are the broad-lined SN Ic (SN Ic-BL). Conversely, SN II are sometimes seen with exceptionally narrow lines. These are the SN IIn, which result from interaction between the ejecta and circumstellar matter. SN Ia are a distinct class whose spectra are characterized by the absence of hydrogen and the presence of a broad absorption feature at 6150Å that is attributed to Si. Unlike all the others, they are attributed to thermonuclear explosions in white dwarfs.

Spectra of the SN are reported by their discoverers or, in many cases, by independent teams. The CfA Supernova program aims to obtain spectra of all the SN north of -20° and brighter than 18th mag (e.g., Matheson et al. 2008), following up discoveries made by amateurs and by programs like the Lick Observatory Supernova Search (LOSS; Filippenko 2003). Programs with the MMT, Magellan, and Gemini pursue fainter SN discoveries from the wide-field PAN-STARRS survey (Kaiser et al. 2010). The Palomar Transient Factory (PTF) (Law et al. 2009), a galaxy-impartial search with the 1.2m Oschin Telescope begun in 2009, has discovered and spectroscopically classified more than a thousand SN. Supernova classifications have become more refined over time and the brief reports in IAU Circulars or in catalogs may need to be revis-

pkelly3@stanford.edu

¹ Kavli Institute for Particle Astrophysics and Cosmology, Stanford University, 382 Via Pueblo Mall, Stanford, CA 94305² SLAC National Accelerator Laboratory, 2575 Sand Hill Rd, Menlo Park, CA 94025³ Harvard-Smithsonian Center for Astrophysics, 60 Garden St., Cambridge, MA 02138³ Harvard-Smithsonian Center for Astrophysics, 60 Garden St., Cambridge, MA 02138⁵ $H_0 = 70 \text{ km s}^{-1} \text{ Mpc}^{-1}$

TABLE 1
GALAXY-IMPARTIAL SAMPLE CONSTRUCTION

Criterion	II	IIf	Ib	Ic	Ic-BL
CC/Asiago+PTF/ $z < 0.15$	116	10	8	16	9
Discovered 1990-Present	116	10	8	16	9
Confident Spec. Confirmation	113	9	8	14	9
Not Ca-rich	113	9	8	14	9
SN Position	113	9	8	14	9
DR8 Imaging Footprint	97	9	8	9	9
Sufficient Coverage	94	8	8	9	9
No Host Detected	91	6	7	9	9
No Bright Star	90	6	7	8	9
No SN Contamination	79	5	7	7	9
Host Fiber	41	1	3	5	4
No AGN Contamination	34	1	3	5	4

NOTE. — See Table 2 description.

ited as new varieties are defined. For this reason, it will be valuable to archive spectra for future analysis, not just present the classification in an IAU Circular. The CfA spectra, and a collection of other spectra organized by the University of Oklahoma SUSPECT database are presently available online^{6,7}.

With the uniform spectroscopy and $u'g'r'i'z$ imaging of the SDSS, we study the environments of the most populous SN types, identifying a series of strong patterns for stripped-envelope SN types. Section 2 describes the data. Section 3 details the construction of the SN sample, classification of the SN, explains how we categorize SN surveys, and scrutinizes SN discoveries for type-dependent biases. We distinguish between the methods of SN discovery and test hypotheses using only targeted or only galaxy-impartial SN. For a number of two-sample comparisons, patterns only have statistical significance when we merge these two samples, but we find reason in Section 3 to believe that any bias introduced by this combination does not dominate the conclusions we draw. The measurement of host galaxy photometry and spectroscopic oxygen abundances is described in Section 4, our statistical method is described in Section 5, and Section 6 presents the results of our analysis. We compare the relative rates of stripped-envelope SN to Type II with increasing host metallicity to model predictions in Section 7. Section 8 presents a discussion of potential systematic effects. Finally, we discuss our results in Section 9 and present conclusions in Section 10.

2. DATA

The imaging component of the SDSS DR8 spans 14555 square degrees and consists of 53.9 second $u'g'r'i'z$ exposures taken with the 2.5m telescope at Apache Point, New Mexico. Each frame consists of a 2048 x 1498 pixel array that samples a 13.5' x 9.9' field. The complementary fiber SDSS DR8 spectroscopic survey covers a 9274 square degree subset of the DR8 imaging footprint. Objects detected at greater than 5σ , selected as extended, and with r' -band magnitudes brighter than 17.77 comprise the main galaxy sample for spectroscopic targeting. When the r' -band 3" fiber magnitude is fainter than 19 magnitudes, fiber targets must meet additional criteria, and physical constraints limit adjacent fibers

⁶ <http://www.cfa.harvard.edu/supernova/SNarchive.html>

⁷ <http://suspect.nhn.ou.edu/~suspect/>

TABLE 2
TARGETED SAMPLE CONSTRUCTION

Criterion	II	IIf	Ib	Ic	Ic-BL
CC/Asiago+PTF/ $z < 0.15$	577	46	70	109	11
Discovered 1990-Present	485	45	61	104	11
Confident Spec. Confirmation	466	40	58	96	11
Not Ca-rich	466	40	57	96	11
SN Position	454	40	57	93	11
DR8 Imaging Footprint	246	23	32	50	9
Sufficient Coverage	233	20	30	49	8
No Host Detected	233	20	30	49	8
No Bright Star	229	20	29	49	8
No SN Contamination	203	18	27	38	7
Host Fiber	114	16	14	25	5
No AGN Contamination	90	13	11	24	5

NOTE. — SN remaining of each spectroscopic type after applying inclusion criteria. (1) SN collected in the Asiago Catalog updated through 2010 November 7 with $z < 0.023$ for targeted discoveries (and, for Table 1, $z < 0.08$ Asiago galaxy-impartial discoveries combined with the 72 Palomar Transient Factory (PTF) core-collapse SN discoveries from March 2009 through March 2010 (Arcavi et al. 2010)) and not classified as Type Ia; (2) SN discovered during period 1990-present; (3) Asiago catalog or PTF SN classification not accompanied by ('?'; ambiguous identification) or ('::'; type inferred from light curve not spectrum); (4) calcium-rich SN 2000ds, SN 2003dg, SN 2003dr, and SN 2005E are grouped apart from other SN (Ib+Ic) because of their potentially distinct progenitor population; (5) SN position coordinates in the host galaxy; (6) inside SDSS DR 8 imaging footprint; (7) retrieved SDSS images collectively cover host galaxy without header issue; (8) host galaxy not detected (SN 2006jl (IIn); SN 2006lh (II); SN 2007fl (II); SN 2008bb (II); SN 2008it (IIn); SN 2009dv (IIP); SN 2009lz (IIP); SN 2009ny (Ib); PTF09gyp (IIf)); (9) no contamination from nearby bright stars; (10) no contamination from residual SN light, the sample used for photometry measurements; (11) an SDSS host fiber available and sufficient S/N to classify using BPT diagram, used for extinction measurements; (12) no AGN contamination in SDSS spectrum. Two SN-LGRB had $z < 0.08$ (SN 1998bw and SN 2006aj), and only the host of SN 2006aj was inside the SDSS DR8. The middle and bottom sections of the Table correspond to the 'Photometry' and the 'Spectroscopic' samples, respectively, subsets of the SN remaining after the 'No Host Detected' criterion is applied.

to be no closer than 55" (Strauss et al. 2002) in a single fiber mask. Because of their large angular sizes, nearby galaxies were often 'shredded' into multiple objects by the SDSS object detection algorithm [see Fig. 9 of Blanton et al. 2005], and many of these galaxies were targeted in multiple locations with fibers. Wavelength coverage of the SDSS spectrograph extends from 3800 to 9200 Å. Exposures typically are a total of 45 minutes taken in three separate 15 minute exposures.

3. SAMPLE

We assemble our SN samples from discoveries collected in the Asiago catalog (Barbon et al. 1999) through 2010 November 6 and 72 Palomar Transient Factory (PTF) core-collapse SN discoveries from March 2009 through March 2010 (Arcavi et al. 2010). Eight of the SN in the Asiago catalog (all Type II SN) are also among the Arcavi et al. 2010 PTF SN (IAU/PTF: 09ct/09cu; 09bk/09t; 09bj/09r; 09bl/09g; 09ir/09due; 09nu/gtt; 10K/09icx; 10Z/10bau).

3.1. Excluding SN Contamination

We consider images taken during the period from 3 months before to 12 months after discovery to be potentially contaminated by SN light. Arcavi et al. 2010 do

not report the exact discovery dates of PTF SN, so, for these SN, the contamination window begins three months before the start and ends 12 months after the completion of the search period.

To assemble SDSS frames of each SN host, we first queried the SDSS SkyServer for any frames within 9.75' of the host galaxy center. If none was available without possible contamination from SN light (even with partial coverage not including from the field center), we instead assembled and constructed mosaics from potentially contaminated images. Such mosaics were used only to measure the deprojected offsets of SDSS spectroscopic fibers and the SN site in each host galaxy. We note that a small number of images retrieved from the SDSS server lacked TAN projection header information, making them unusable for our analysis.

3.2. Spectroscopic Classes

Our previous work has shown that SN Ic are more strongly associated with bright regions in their host galaxies' g' -band light than are SN Ib (Kelly et al. 2008), indicating that they have a distinct progenitor population, so we group them separately in this analysis. SN IIb and SN IIn subtypes are excluded from the "SN II" sample. A single SN-LGRB, SN 2006aj, meets the sample criteria, but we consider it separately from SN Ic-BL discovered through their optical emission (which have no associated LGRB). Today's gamma-ray searches are not sensitive to normal SN explosions.

We exclude SN 2006jc, a peculiar SN Ib with narrow helium emission lines and an underlying broad-lined SN Ic spectrum (e.g., Foley et al. 2007; Pastorello et al. 2007), from our SN Ib statistical sample. The helium emission may reflect the collision of ejecta with a helium-rich circumstellar medium.

From a comprehensive set of spectra, we update the classification of SN 2005az. This SN was discovered approximately seventeen days before maximum and spectroscopically classified three days after discovery as a SN Ic by Quimby et al. 2005a. The Nearby Supernova Factory, from a spectrum taken five days after discovery, suggested it as a Type Ib (Aldering et al. 2005). SNID (Blondin & Tonry 2007) cross correlation, applied to 24 spectra taken by the CfA Supernova Group from approximately ten days before to twenty-five days after maximum, shows that it was a Type Ic explosion.

We group calcium-rich SN 2000ds, SN 2003dg, SN 2003dr, and SN 2005E separately from other SN (Ib+Ic) because of their potentially distinct progenitor population.

We exclude SN IIn imposters (e.g., Van Dyk et al. 2000; Maund et al. 2006), a group which includes SN 1997bs, SN 1999bw, SN 2000ch, and SN 2001ac.

3.3. Classification of SN as Type IIb

While spectra taken over several epochs are necessary to observe the spectroscopic transition that defines SN IIb, such follow up is not always available. Fortunately, the spectra of Type IIb SN similar to SN 1993J are sufficiently distinctive that cross correlation with spectroscopic templates (e.g., the "Supernova Identification code" (Blondin & Tonry 2007)), has been able to identify substantial numbers of explosions as Type IIb from

a single spectrum. Although classifications based on a single spectrum may overlook examples of SN IIb, the Type IIb explosions they do identify should be reliable.

3.4. Classification of SN as Type Ib/c SN

The Asiago catalog entries sometimes have less information than the IAU Circulars and published papers. For example, SN 1997dq and SN 1997ef were listed in the Asiago catalog (as of November 2010) as "Type Ib/c" while Matheson et al. 2001 and Mazzali et al. 2004 identified them as SN Ic-BL. Motivated by these examples, we searched the circulars to see whether additional information was available. Despite making note of the presence or absence of helium more than ten days after the explosion, some authors report a Type Ib/c classification. These authors may feel that a SN Ib/c classification was sufficiently precise while, in other cases, they may have wanted to emphasize peculiar spectroscopic characteristics. An example is SN 2003A which was classified as a Type Ib/c by Filippenko & Chornock 2003 who noted that "[w]eak He I absorption lines are visible, but the overall spectrum resembles that of type-Ic supernovae."

Classifications by the Nearby Supernova Factory (Aldering et al. 2002; Wood-Vasey et al. 2004) reported in circulars include an unusually high percentage of Type Ib/c. The high fraction of SN Ib/c reported by the Nearby Supernova Factory survey is hard for us to assess without being able to see the spectra or use impartial classification techniques. We have therefore excluded SN discovered by the Nearby Supernova Factory from our statistical sample.

3.5. Galaxy-Impartial and Targeted SN Surveys

We measure the host galaxy properties of SN discovered by both *targeted* surveys, which aristocratically discover almost all their SN in luminous galaxies, as well as *galaxy-impartial* surveys, which democratically scan swaths of sky without special attention to specific galaxies. Galaxy-impartial surveys generally employ larger telescopes (e.g., the SDSS 2.5m; the PTF 1.2m) than targeted surveys (e.g., the KAIT 0.76m), have fainter limiting magnitudes, and image much greater numbers of low-mass galaxies. The SN harvested by galaxy-impartial surveys are found in host galaxies that are not apparently bright or nearby (and are not in bright galaxy catalogs). For example, in our sample, 31% (40/130) of galaxy-impartial SN but only 3.4% (13/385) of targeted SN have host galaxy masses smaller than $10^9 M_\odot$.

3.6. Identifying Galaxy-Impartial Discoveries

We used the Discoverer column from the IAU classification⁸ to determine the provenance of each SN. There are relatively few galaxy-impartial discovery teams, because discovering substantial numbers of SN by impartially scanning the sky requires significant dedicated observing time and investment in data processing. Any SN whose discovery team we did not identify as part of a galaxy-impartial search effort, including amateur discoveries, was considered a targeted discovery.

Surveys that we considered galaxy-impartial: Catalina Real-Time Sky Survey and Siding Spring Survey

⁸ <http://www.cfa.harvard.edu/iau/lists/Supernovae.html>

TABLE 3
MEDIAN REDSHIFTS FOR EACH SN TYPE

Survey Type	II	IIn	IIf	Ib	Ic	Ic-BL	Ib/c
Galaxy-Impartial	0.045	0.041	0.033	0.05	0.053	0.05	0.03
Targeted	0.016	0.017	0.013	0.015	0.014	0.016	0.017

NOTE. — Median redshifts of each SN type in the galaxy-impartial and targeted samples.

(Djorgovski et al. 2011), La Sagra Sky Survey, PAN-STARRS (Kaiser et al. 2010), Palomar Transient Factory (Law et al. 2009), ROTSE (Yost et al. 2006), ESSENCE (Miknaitis et al. 2007), Palomar-Quest (Djorgovski et al. 2008), SDSS-II (Sako et al. 2005), Supernova Legacy Survey (Astier et al. 2006), Supernova Cosmology Project (Perlmutter et al. 1999), Near Earth Asteroid Tracking Program (Pravdo et al. 1999), High-Z Supernova Search (Riess et al. 1998), EROS Hardin et al. 2000, GOODS (Dickinson et al. 2003), Deep Lens Survey (Wittman et al. 2002), and, except for discoveries in targets IC342, M33, M74, M81, NGC 6984, and NGC 7331, the Texas Supernova Search (Quimby et al. 2005b).

3.7. Luminosity Functions, Light Curves, and Detection

Any type-dependent luminosity differences which influence the relative visibility of the SN types are a potential concern, because SN surveys may image different potential host galaxy populations at increasing redshift or with varying depth. For example, Leaman et al. 2011 report a Malmquist effect among the galaxies targeted by LOSS where more distant galaxies are, on average, more luminous. Detection efficiencies that depend on redshift and type could result in false correlations between host galaxy properties and SN type.

Table 4 shows the mean peak absolute magnitudes (before correction for host galaxy extinction) of the core-collapse SN species studied by Li et al. 2011b (LOSS) and Drout et al. 2010 (Palomar 60"). Drout et al. 2010 found that SN Ic-BL are intrinsically brighter explosions than normal Type Ic explosions. Besides SN Ic-BL, there is no strong or unanimous support for differences among the SN types. Although Li et al. 2011b found some evidence that SN Ib and SN Ic have different mean intrinsic luminosities, Drout et al. 2010 did not find a similar indication.

Modest differences among the mean luminosities of SN species do not necessarily correspond to strong differences among detection efficiencies, given redshift limits and survey cadence. Intrinsic SN luminosities vary by at least several magnitudes, even among SN of the same spectroscopic type. Li et al. 2011b found, for example, that the SN (Ib+Ic) luminosity function has a standard deviation of 1.24 mag and that the SN II luminosity function has a standard deviation of 1.37 mag.

3.7.1. Redshift Upper Limits for Targeted and Galaxy-Impartial Samples

To avoid misleading correlations introduced by the sample selection, we exclude SN discovered at redshifts where these SN surveys could only detect SN Ib, SN Ic, or SN II if they were brighter than average. Li et al. 2011b reported the mean peak luminosities of SN (Ib+Ic),

-16.09 ± 0.23 mag, and SN II, -16.05 ± 0.15 mag, discovered by LOSS. While LOSS survey observations are taken without a filter, the response function peaks in the *R*-band (Li et al. 2011b). For LOSS, which contributes 42% of our targeted sample, Leaman et al. 2011 find a median limiting magnitude of 18.8 ± 0.5 , corresponding to a detection limit of $z = 0.023$ for SN (Ib+Ic) and SN II. We use this redshift as the upper limit for our targeted SN sample. Table 3 presents the median redshifts for each SN type.

Dilday et al. 2010 report a ~ 21.5 mag *r'*-band detection limit for the SDSS-II survey, which accounts for 33% of the galaxy-impartial sample. For our sample of galaxy-impartial discoveries, the redshift upper limit is $z = 0.08$, corresponding to the SDSS-II detection limit. The PTF, accounting for 32% of galaxy-impartial SN, has a limiting *R*-band magnitude of ~ 20.8 mag which corresponds to an upper detection limit of $z = 0.056$.

Varying the upper redshift limit for galaxy-impartial and targeted SN discoveries (e.g., from $z = 0.023$ to $z = 0.02$ or $z = 0.06$) does not alter the type-dependent trends we find.

3.8. Galaxy-Impartial SN Discoveries as a Test

Except for cosmic evolution, low-redshift galaxy-impartial surveys image the same galaxy populations at increasing redshift. Therefore, the SN populations that explode within the field of view of galaxy-impartial surveys at each redshift to $z < 0.15$ should be unvarying, with constant fractions of each SN type, so the mix of SN types as a function of redshift reflects the efficiency of the survey for each type at each redshift.

Figure 1 plots the cumulative redshift distributions of core-collapse SN reported to the IAU by galaxy-impartial surveys with $z < 0.15$. We extend the redshift upper limit beyond the $z = 0.08$ galaxy-impartial limit to compile a larger sample of SN discoveries. The samples of some SN species are modest, but this plot provides no suggestion that these surveys are, in the aggregate, more or less sensitive to the explosions of SN II, SN IIf, SN IIn, SN Ib, SN Ic, and SN Ic-BL with increasing redshift. Besides their targeting patterns, galaxy-impartial and targeted surveys are generally alike, so a reasonable assumption is that any type-dependent luminosity differences also do not strongly affect our targeted SN sample.

3.9. Approximately Consistent Efficiency and Combination of Samples

We have found some evidence that, for each galaxy imaged within the redshift limit, the probability of detecting a SN is independent of the spectroscopic type of the SN. This implies that differences among the host properties of detected SN largely reflect the environmental preferences of each SN type, not primarily type-dependent

TABLE 4
SN LUMINOSITY FUNCTIONS

Survey	II	IIIn	IIb	Ib	Ic	Ic-BL	Ib+Ic
LOSS (Li et al. 2011b)	-16.05 ± 0.17	-16.86 ± 0.59	-16.65 ± 0.40	-17.01 ± 0.17	-16.04 ± 0.31	...	-16.09 ± 0.23
P60 (Drout et al. 2010)	-17.0 ± 0.7	-17.4 ± 0.4	-18.3 ± 0.6	...

NOTE. — Estimates of the mean luminosities of the SN types by Li et al. 2011b and Drout et al. 2010. The LOSS and the P60 samples, respectively, are constructed differently, but differences between the mean luminosities of the SN species should be approximately consistent for these surveys. Li et al. 2011b favor a much larger difference between SN Ib and SN Ic luminosities than that found by Drout et al. 2010. SN Ic-BL may be more intrinsically luminous than SN Ic. Luminosities above are before correction for extinction, for studying SN detection efficiency.

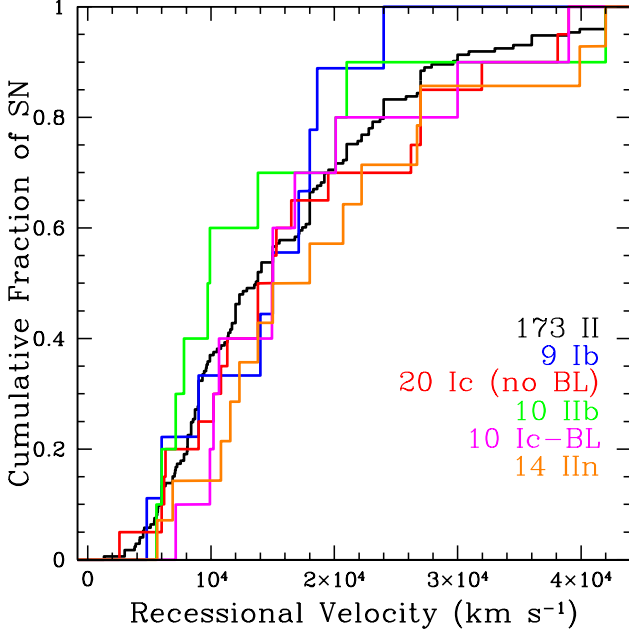


FIG. 1.— Recessional velocities of SN discovered by galaxy-impartial surveys. To increase sample size, the plot includes discoveries to $z = 0.15$, a higher upper limit than the $z = 0.08$ galaxy-impartial sample limit. Except for cosmic evolution, low-redshift galaxy-impartial surveys image the same galaxy populations at increasing redshift. The samples of some SN species are modest, but this plot provides no suggestion that these surveys are, in the aggregate, more or less sensitive to the explosions of SN II, SN IIb, SN IIIn, SN Ib, SN Ic, and SN Ic-BL with increasing redshift.

luminosity selection effects. We can therefore combine the galaxy-impartial and targeted samples with reasonable confidence before we compare host galaxy properties.

4. METHODS

4.1. SDSS Imaging Processing

The WCS provided in SDSS DR8 **frame*.fits** headers is a TAN approximation to the **asTrans*.fits** full astrometric solution and has subpixel accuracy (private communication; M. Blanton), an improvement over the astrometric solution provided in DR7 **fpC*.fit** headers. We used SWarp (Bertin et al. 2002) to register and resample SDSS images of each host galaxy to a common pixel grid and coadded SDSS images in the $u'g'r'i'z'$ bands. The SDSS DR8 **frame*.fits** images also feature an improved background subtraction (in comparison to DR7 **fpC*.fit** images). The DR8 background level is estimated from a spline fit across consecutive, adjacent frames from each drift scan, after masking objects in each image.

4.2. Galaxy Photometry and Stellar Mass

Host galaxy images were used to measure the color of the stellar population near the site of each SN, estimate each host's stellar mass, a proxy for chemical enrichment (e.g., Tremonti et al. 2004), and compute the deprojected host offsets of SN and SDSS spectroscopic fibers. The SExtractor measurement **MAG_AUTO**, corresponding to the flux within 2.5 Kron (1980) radii, was used to estimate host galaxy stellar mass-to-light ratio (M/L) through fits with spectral energy distributions (SEDs) from PEGASE2 (Fioc & Rocca-Volmerange 1997, 1999) stellar population synthesis models using the appropriate SDSS instrumental response function. An estimate of the stellar mass was then computed: $M = M/L \times L$ where L is the galaxy's absolute luminosity. See Kelly et al. 2010 for a detailed description of the star formation histories used.

We then estimated the host galaxy's color near the SN location using two techniques. The first and more simple method was to extract the $u'g'r'i'z'$ flux inside of a circular aperture with 300 pc radius centered on the SN location, after subtracting the median of the peripheral background regions. While this technique is straightforward, apertures centered at the sites of SN at large host offsets or found in low-luminosity hosts had low S/N, especially in the u' and z' bands. The primary intent of the second method was to obtain higher S/N u' -band flux measurements near the sites of SN, in particular near the sites of the SN with faint hosts. To identify g' -band pixels with $S/N > 1$, we searched the SExtractor segmentation map generated with settings **DETECT_THRESH=1** and **DETECT_MINAREA=10** (minimum of 10 contiguous pixels with $S/N > 1$). The 20 pixels closest to the SN location contained in the g' -band segmentation maps define the aperture for measurements of u' - z' color and u' -band surface brightness. We correct for Galactic reddening using the Schlegel et al. 1998 dust maps.

We note that each K-corrected magnitude which we computed using **KCORRECT** (v. 4.13) (Blanton & Roweis 2007) reflects the shape of the best-fit SED and therefore the full set of $u'g'r'i'z'$ measurements. Consequently, even if the u' and z' fluxes are noisy, the K-corrected u' - z' color is still a useful indicator of the shape of the SED that best fits less noisy $g'r'i'$ fluxes.

4.3. Selecting SDSS Spectroscopic Fibers

To identify SDSS fibers that coincide with a host galaxy, we searched inside a catalog available online from an MPA-JHU collaboration⁹ for fibers that fell within an

⁹ <http://www.mpa-garching.mpg.de/SDSS/DR8/>

aperture with radius $(1.65/z)''$ placed on the host center and with redshifts that agree with that of the SN. For an object in the Hubble flow, this angle corresponds to a physical distance of approximately 34 kpc. At $z = 0.03$, for example, this radius subtends a $55''$ angle. If the g' -band SExtractor segmentation map ID at the fiber location was the same as the ID of the SN host galaxy, the fiber was considered a match to the galaxy after a visual check. The deprojected normalized offset of the fiber was then calculated by computing the offset at each pixel in the $3''$ fiber aperture and averaging these offsets weighted by each pixel's g' -band counts.

4.4. AGN Activity

The hard ionizing continuum of AGN emission affects the relative strengths of the strong optical nebular emission lines, making a nuclear spectrum a useful indicator of activity. The patterns associated with AGN activity are significantly degenerate with variation in oxygen abundance, however, so AGN contamination precludes metallicity measurements.

We use the classifications of fiber spectra as star forming, low S/N star forming, composite, AGN, or low S/N AGN made available by the MPA-JHU group following Brinchmann et al. 2004. That analysis uses each spectrum's position on the Baldwin et al. 1981 (hereafter BPT) diagram of $[\text{O III}] \lambda 5007/\text{H}\beta$ and $[\text{N II}] \lambda 6584/\text{H}\alpha$ line ratios.

4.5. Extinction Estimated from Balmer Ratios

From the fiber spectra (closest in deprojected offset to the SN sites), we estimate host galaxy reddening A_V using the Balmer decrement ($\text{H}\alpha/\text{H}\beta$), assuming the $R_V=3.1$ Cardelli et al. 1989 extinction law. Following Osterbrock 1989, we assume a Case B recombination ratio of 2.85 when spectra are classified as star forming or low S/N star forming and a ratio of 3.1 when spectra are classified as composite, AGN, or low S/N AGN.

4.6. Metallicity and Specific SFR Measurements

Our analysis uses both (a) abundances and specific star formation rate estimates available from the MPA-JHU collaboration for SDSS fiber spectra and (b) abundances we compute using the Pettini & Pagel 2004 metallicity calibration. We only use galaxies with $\text{S/N} > 3$ $\text{H}\beta$, $\text{H}\alpha$, $[\text{N II}] \lambda 6584$, and $[\text{O III}] \lambda 5007$, as designated by the MPA-JHU analysis. For abundance measurements, we only analyze spectra classified as star forming. For specific SFR estimates, we use star forming, composite, and AGN spectra.

4.6.1. MPA-JHU Metallicity and Specific SFR

To extract an oxygen abundance and specific SFR from a spectrum, the MPA-JHU collaboration first uses Charlot & Longhetti 2001 stellar population synthesis and photoionization models to calculate an extensive library of line strengths spanning potential effective gas parameters including gas density, temperature, and ionization as well as the dust-to-metal ratio. Then galaxy $[\text{O II}]$, $\text{H}\beta$, $[\text{O III}]$, $\text{H}\alpha$, $[\text{N II}]$, and $[\text{S II}]$ optical nebular emission lines are fit simultaneously with the library and used to compute metallicity and specific SFR likelihood distributions. Here we use the median of these

distributions as the oxygen abundance and specific SFR estimates.

When AGN contaminate emission lines, metallicity estimates are not possible but the MPA-JHU group uses the strength of the 4000Å break [see Figure 11 of Brinchmann et al. 2004] and the ratio $\text{H}\alpha/\text{H}\beta$ to estimate the specific SFR¹⁰.

4.6.2. Pettini and Pagel Metallicity

Since we have no prejudice about which emission-line method is most correct, we have also computed abundances using the Pettini & Pagel 2004 (hereafter PP04) prescription. This is based on the relative line strengths of $\text{H}\beta$, $\text{H}\alpha$, $[\text{N II}] \lambda 6584$, and $[\text{O III}] \lambda 5007$, after correcting for dust emission. The PP04 indicator relies on lines relatively close in wavelength, reducing its sensitivity to uncertainty in the extinction correction and does not require the $[\text{O II}] \lambda 3727$ line, which falls beyond the blue sensitivity of the SDSS spectrograph for objects at $z < 0.02$.

Our measurements trace the Kewley & Ellison 2008 PP04 mass-metallicity relation of SDSS galaxies when stellar mass is plotted against 'central' metallicity for galaxies in the Hubble flow ($z > 0.005$). Fibers were considered 'central' if their deprojected offset was less than 0.35 the half-light radius or were closer than 2 kpc to the galaxy center.

4.7. Comparison of Host Abundance Proxies

Oxygen abundances measured from fibers centered on the host galaxy nucleus are, on average, only 0.01 dex (T04) greater than the abundance inferred from the stellar mass with the Tremonti et al. 2004 $M-Z$ relation, with a scatter of 0.14 dex. If we instead select fibers closest in host offset to SN explosion sites, spectroscopic abundances are 0.053 dex (T04) less than abundances estimated from stellar masses with a scatter of 0.16 dex.

5. STATISTICAL METHOD

5.1. Kolmogorov-Smirnov Statistic

In the following sections, we test the null hypothesis that two samples are drawn from a single underlying distribution using the Kolmogorov-Smirnov (KS) test. The KS test statistic is defined as $D = \sup_x |F_1(x) - F_2(x)|$, the maximum difference between the samples' cumulative distribution functions, where $F_n(x) = \frac{1}{n} \sum_{i=1}^n I_{X_i \leq x}$. The KS distribution is the distribution of the test statistic D , given the null hypothesis that two distributions are identical. The p-value is the probability of observing a value of the test statistic, D , more extreme than the observed value of D given the null hypothesis that the two samples are drawn from a single underlying distribution. Low p-values ($< 5\%$) are significant evidence that the underlying distributions are distinct.

When two independent samples are drawn from the same distribution, there is, by definition, a 5% random chance of obtaining a p-value less than 5%. If we were to make, for example, twenty comparisons among samples drawn from identical distributions, one misleading $p < 5\%$

¹⁰ <http://www.mpa-garching.mpg.de/SDSS/DR7/sfrs.html>

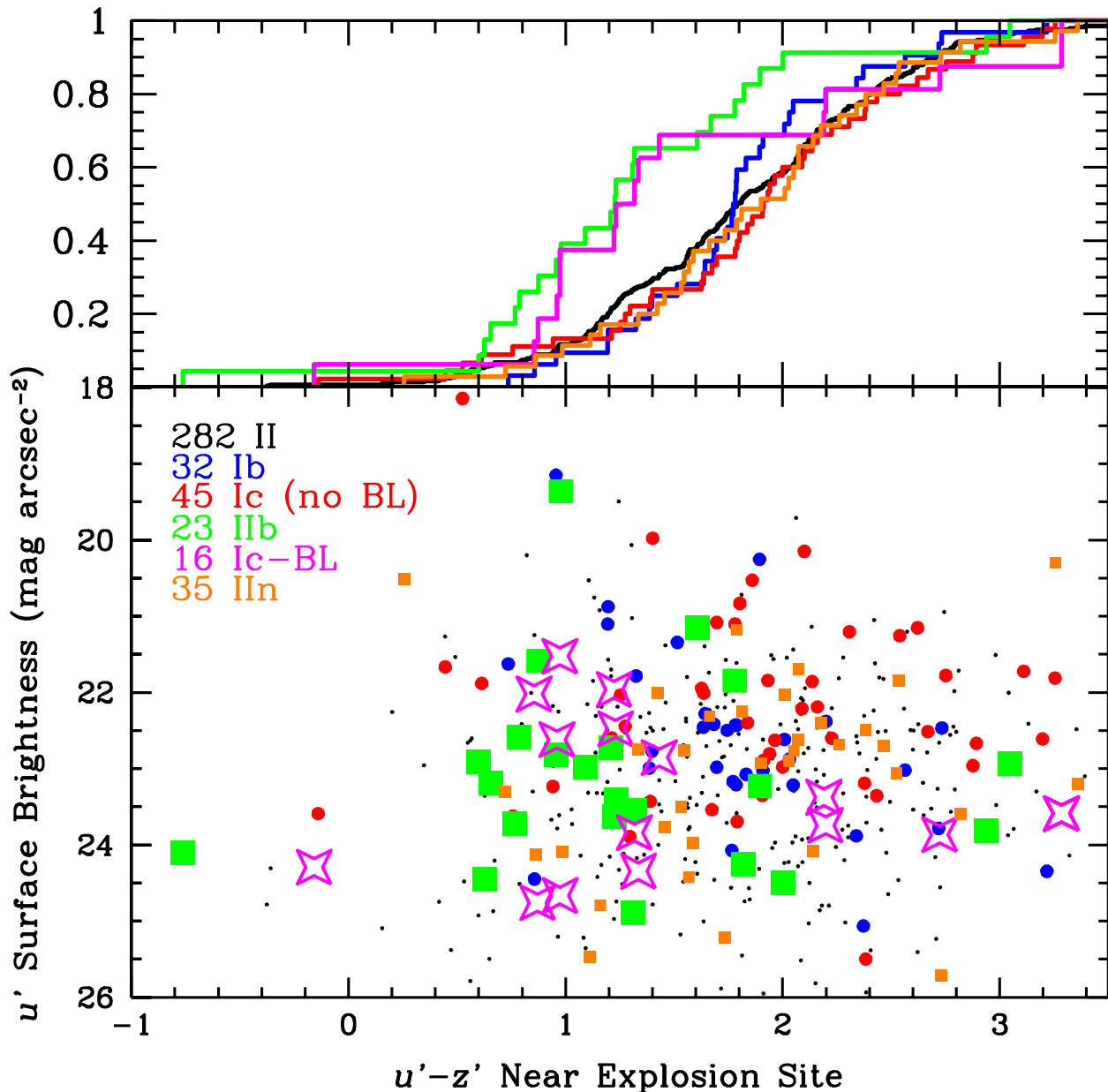


FIG. 2.— Host galaxy $u'-z'$ color versus u' surface brightness near SN location. The top panel plots the fraction of SN of each type with environments bluer than the horizontal axis coordinate. SN IIb environments are bluer than SN Ib, SN Ic, and SN II environments ($p=0.2\%$, 0.5% , and 0.3% , respectively), and SN Ic-BL environments are bluer than those of SN Ib, SN Ic, and SN II ($p=2.3\%$, 2.1% , and 1.7% , respectively). SN Ib and SN Ic explode in regions with higher u' -band surface brightness than do SN II ($p=2.4\%$ and 0.3% , respectively), and SN Ic sites have higher u' -band surface brightnesses than SN Ic-BL locations (0.7%). The aperture is the 20 host pixels with $S/N > 1$ in g' band nearest the SN location.

difference would occur by chance on average. The number of independent comparisons we make in this paper should therefore be taken into account when comparisons yield p-values of modest significance ($p \sim 5\%$). We note that the host properties we measure are correlated (e.g., host color and metallicity), so independent comparisons are fewer than the total number of comparisons.

6. RESULTS

Instead of placing the numerical values of all statistical Kolmogorov-Smirnov (KS) tests in the following descriptions of results, we instead list many of them in Table 5, which includes comparisons for all types, and Table 6, which includes comparisons for SN IIb and SN Ic-BL, re-

stricted to only targeted and only galaxy-impartial samples. Table 7 contains the measurements of the SN host galaxies.

6.1. Host Color and u' Surface Brightness Near Explosion Site

As can be seen in Figure 2, SN IIb and SN Ic-BL erupt in exceptionally blue environments, while high u' -band surface brightness is typical of SN Ib and SN Ic sites. This plot shows $u'-z'$ color versus u' -band surface brightness, measured inside an aperture consisting of the 20 pixels closest to the SN site with g' -band $S/N > 1$.

The $u'-z'$ color near the site of SN 2006aj, the SN-

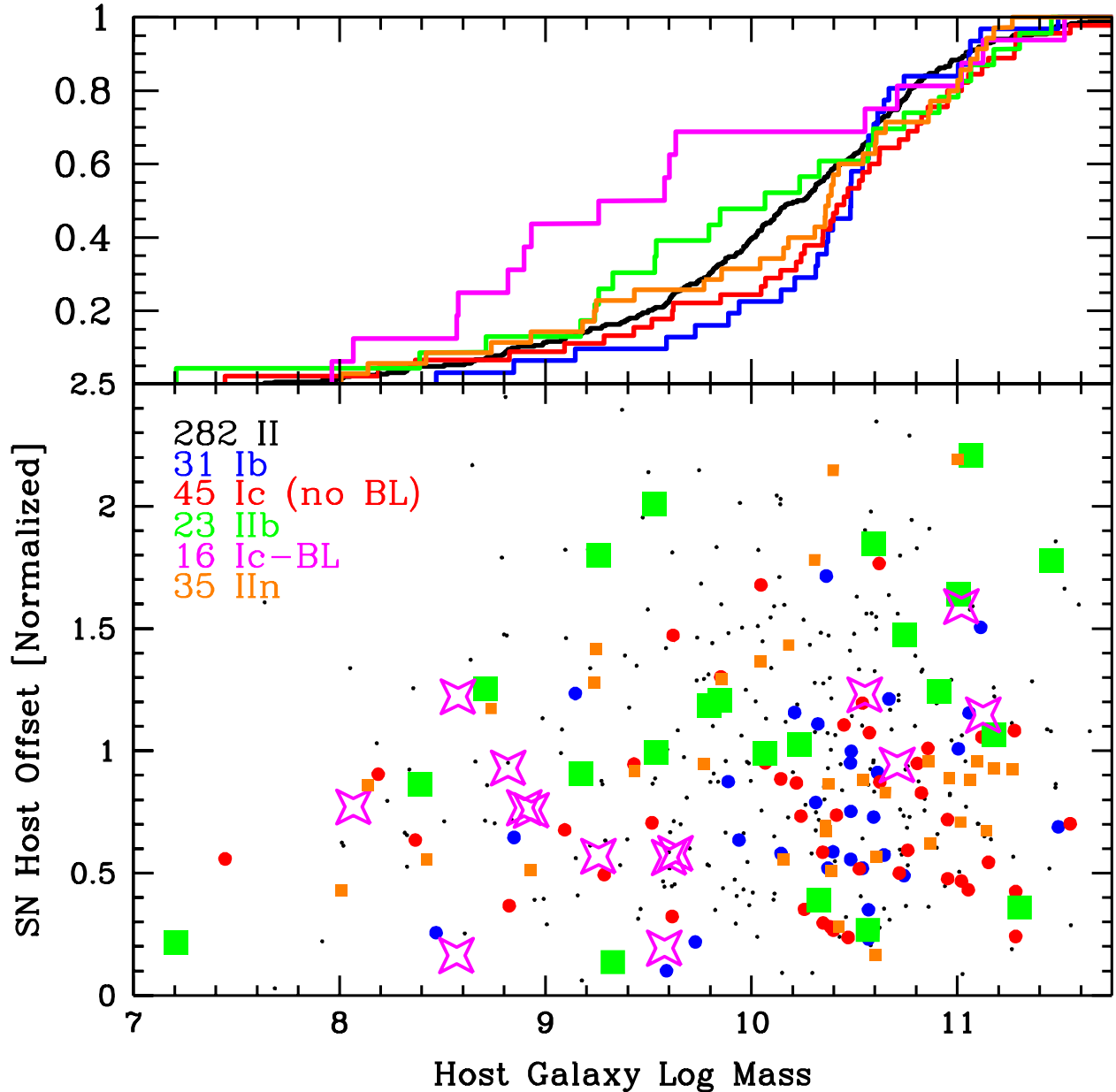


FIG. 3.— Stellar masses of host galaxies versus SN host offset, deprojected and normalized by host g' -band half-light radius. The top panel plots the fraction of each SN type with hosts less massive than the horizontal axis coordinate. SN Ic-BL are found in significantly less massive galaxies than are the SN Ib, SN Ic, or SN II ($p=0.1\%$, 0.8% , and 0.4% , respectively). Host galaxy stellar masses are estimated from PEGASE fits to $u'g'r'i'z'$ host magnitudes. A two-sample KS test finds evidence ($p=5.1\%$) that SN IIb explode at larger host offsets than SN Ib. SN Ic explode closer to their host centers than SN II ($p=0.2\%$).

LGRB in our sample, was 0.88 mag.

6.2. Host Stellar Mass and SN Host Offsets

Figure 3 helps to explain the exceptionally blue $u'-z'$ color of SN IIb and SN Ic-BL sites and the high u' -band surface brightnesses near SN Ib and Ic sites. At one set of extremes, SN Ic-BL have generally low mass hosts, while SN IIb explode at larger offsets when they occur in galaxies of large masses. At another extreme, SN Ib and especially SN Ic more often occur inside the g' -band half-light radius massive galaxies, sites expected to have redder color and high surface brightness. SN II sites are indifferent, showing no evident preference in color or surface brightness.

Host galaxy mass is a moderately precise (~ 0.1 dex) proxy for chemical abundance (e.g., Tremonti et al. 2004) which does not suffer from the AGN selection effects. The hosts of SN (Ib+Ic), excluding SN Ic-BL, are more massive than SN II hosts.

The host stellar mass of SN 2006aj, the only SN-LGRB in our sample, was $8.0 \times 10^{10} M_{\odot}$. We find with $p=13\%$ that the SN IIc offset distribution is consistent with the SN II host offset distribution.

6.3. Oxygen Abundance Measurements Closest to SN Positions

To probe the metallicities of the core-collapse hosts, we measure oxygen abundance from the fiber spectrum with

TABLE 5
KS P-VALUES FOR COMBINED SAMPLES

Measurement	Figure	Samples	P-value
$u'-z'$	2	Ic-BL vs. Ib, Ic, II	2.3%, 2.1%, 1.7%
...	...	IIb vs. Ib, Ic, II	0.2%, 0.5%, 0.3%
u' SB	2	Ib vs. Ic, II	2.4%, 10%
...	...	Ic vs. II	0.3%
$\log M$	3	Ic-BL vs. II, IIb, Ib, Ic	0.4%, 27%, 0.1%, 0.8%
...	...	IIb vs. II, Ib, Ic	44%, 11%, 23%
...	...	II vs. Ib, Ic, (Ib+Ic)	4.6%, 10%, 0.8%
Offset	3	Ic-BL vs. II, Ib, Ic	77%, 14%, 83%, 52%
...	...	IIb vs. II, Ib, Ic	16%, 5.1%, 0.08%
...	...	II vs. Ib, Ic	21%, 0.2%
T04/PP04	4	II vs. Ib, Ic	31%/0.6%, 0.3%/0.6%
< 3 kpc		Ic-BL vs. Ib, Ic	2.8%/0.4%, 0.2%/0.004%
...		II vs. Ib, Ic	88%/95%, 0.5%/0.2%
SSFR	5	II vs. Ib, Ic, Ic-BL	6.5%, 1.2%, 5.9%
...	...	Ib vs. Ic	2.7%
A_V	6	(Ib+Ic) vs. IIb, II	4.2%, 1.8%

NOTE. — P-values from Kolmogorov-Smirnov two-sample comparisons that include both targeted SN and galaxy-impartial SN discoveries. The two rows below “T04/PP04” show oxygen abundance statistics computed from spectra whose host offsets are within 3 kpc of the SN host offset.

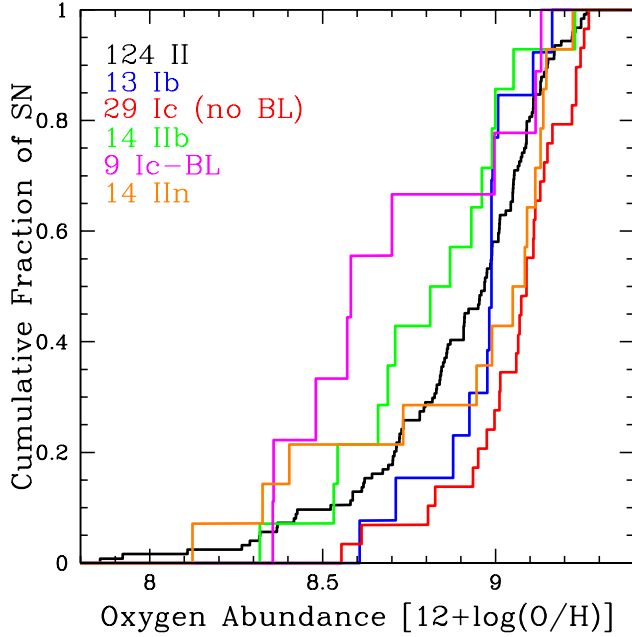


FIG. 4.— Host oxygen abundance measured from SDSS 3” fiber spectrum with host radial offset most similar to that of SN explosion site. While Tremonti et al. 2004 spectroscopic abundances are plotted, we also measure abundances using the Pettini & Pagel 2004 calibration. Even when we consider only SN discovered by galaxy-impartial surveys, we find a statistically significant difference between the SN Ic-BL and the SN Ic host abundance distributions ($p=0.7\%/0.7\%$, respectively for the T04/PP04 calibrations). When we consider only SN discovered by targeted surveys, we find a statistically significant difference between the SN IIb and the SN Ib host abundance distributions ($p=4.7\%/0.6\%$, respectively for the T04/PP04 calibrations).

deprojected offset most similar to the SN offset. SDSS fiber spectra generally target the central regions of host galaxies, with an average host offset in our sample of $0.45 \times r_{\text{half-light}}$. The low metallicities shown in Figure 4 for SN Ic-BL and SN IIb hosts and high metallicities for SN Ic hosts are consistent with the patterns we see among the species’ colors near explosion sites, host offsets, and host masses.

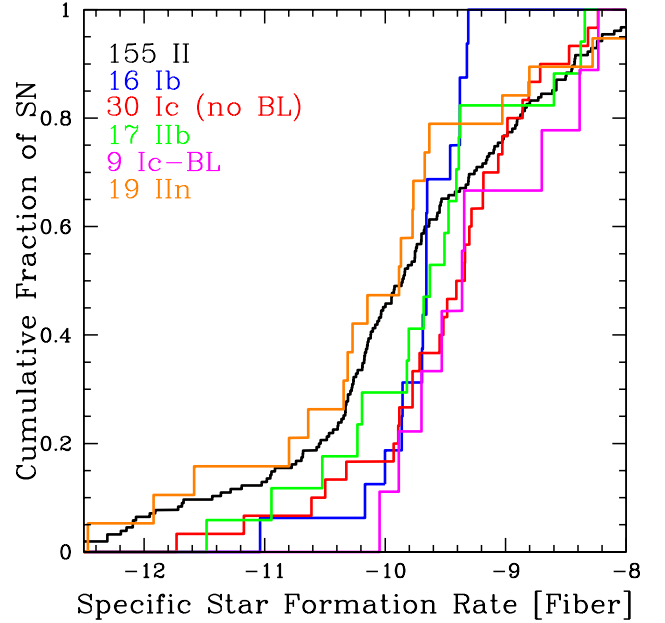


FIG. 5.— Host specific SFR estimated from SDSS 3” fiber spectrum with host radial offset most similar to that of SN explosion site. The sequence of the spectroscopic classes, arranged in order of the loss of the progenitor’s outer hydrogen and helium envelopes (i.e., SN II, SN IIb, SN Ib, SN Ic), exhibit increasing average host galaxy specific SFR ($\text{SFR } M_{\odot}^{-1} \text{ yr}^{-1}$), measured from SDSS fiber spectra. SN Ic hosts have greater specific SFR than SN Ib hosts ($p=2.7\%$), while SN Ib hosts have greater specific SFR than SN II hosts (6.5%). SN Ic-BL hosts have greater specific SFR than SN II hosts (5.9%). SDSS fibers largely sample light within the the host galaxy half-light radius and are often centered on the host galaxy nucleus.

6.3.1. Every Abundance Measurement

For galaxy-impartial discoveries, SN Ic-BL hosts ($n=4$) follow a significantly more metal-poor distribution than the hosts of normal SN Ic ($n=5$; $p=0.7\%/0.7\%$ for T04/PP04 calibrations). Among the hosts of targeted discoveries, host galaxies of SN IIb ($n=13$) follow a significantly more metal-poor distribution than hosts of SN Ib ($n=10$; $p=4.7\%/0.6\%$).

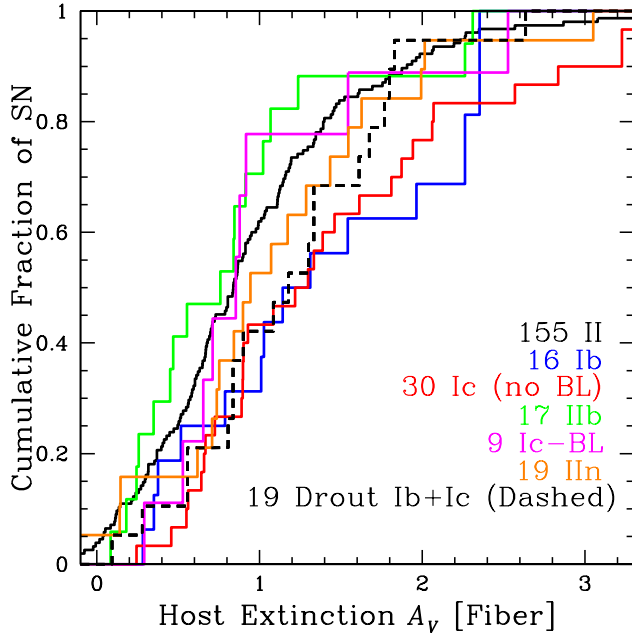


FIG. 6.— Host extinction estimated from 3" SDSS fiber spectrum with host radial offset most similar to that of SN explosion site. There is significant evidence that SN IIb and SN II hosts have less internal extinction than SN (Ib+Ic) host galaxies ($p=4.2\%$ and 1.8% , respectively). The Drouot et al. 2010 SN (Ib+Ic) A_V extinction values estimated along the line of sight to the SN from light curve color and shape are consistent with the values we measure, although the spectroscopic fibers are largely not positioned at the SN site.

TABLE 6
KS P-VALUES FOR DIFFERENT SAMPLES

	Sample	Iib vs. Ib	Ic-BL vs. Ic
$u'-z'$	All SN	0.2% (23, 32)	2.1% (16, 45)
	Targeted	5.5% (18, 25)	9.2% (7, 38)
	Impartial	1.0% (5, 7)	50% (9, 7)
$\log M$	All SN	11% (23, 31)	0.8% (16, 45)
	Targeted	16% (18, 24)	75% (7, 38)
	Impartial	19% (5, 7)	84% (9, 7)
PP04	All SN	1.8% (14, 13)	0.08% (9, 29)
	Targeted	0.6% (13, 10)	14% (5, 24)
	Impartial	16% (1, 3)	0.7% (4, 5)
T04	All SN	14% (14, 13)	0.8% (9, 29)
	Targeted	4.7% (13, 10)	44% (5, 24)
	Impartial	16% (1, 3)	0.7% (4, 5)
Host Offset	All SN	5.1% (26, 34)	52% (17, 58)
	Targeted	5.4% (20, 27)	27% (8, 49)
	Impartial	62% (6, 7)	60% (9, 9)

NOTE. — P-values and sample sizes from Kolmogorov-Smirnov two-sample comparisons that include targeted SN discoveries, galaxy-impartial SN discoveries, or both. The difference between the metallicity distributions of the hosts of Type Ic-BL and Type Ic SN is statistically even when including only SN discovered by galaxy-impartial hosts. The differences between the SN Ib and SN IIb host galaxy $u'-z'$ color distributions as well as host galaxy metallicities are statistically significant when including only SN discovered by targeted surveys.

The SN II host abundance distribution is more metal-poor than that of the SN Ic hosts, but a selection effect may inflate any difference. A higher fraction of SN II ($21\pm3\%$ (42/196)) than SN (Ib+Ic) host spectra ($9\pm4\%$ (4/47)) have the emission line ratios of AGN (see Tables 1 and 2), which makes spectra unusable for abundance

analysis. AGN occur primarily in massive, metal-rich galaxies ($M > 10^{10} M_{\odot}$; Kauffmann et al. 2003), so rejecting AGN spectra removes a higher fraction of metal-rich SN II hosts than of SN Ib/c hosts. A host galaxy with mass $10^{10.5} M_{\odot}$, typical of an AGN host, will have an oxygen abundance of ~ 9 dex (T04) and ~ 8.75 dex (PP04) (e.g., Tremonti et al. 2004).

SN IIc hosts follow a similar distribution to that of the entire SN II sample ($p=37\%/55\%$).

6.3.2. When Fiber and SN Host Offsets Are Similar

Most galaxies have metallicity gradients, with abundance declining away from the galaxy center. Van Zee et al. 1998 found, for example, a mean radial abundance gradient of -0.052 dex kpc^{-1} for a sample of 11 NGC host galaxies. To assemble improved proxies for metallicity at the SN location, we selected fibers whose deprojected host offset (away from the galaxy center) was within 3 kpc of that of a SN.

Among these fibers, the SN Ic-BL host spectra are significantly more metal-poor than both the SN Ib and SN Ic spectra. More qualified evidence exists that SN Ic spectra are more metal-rich than SN Ib spectra ($p=2.4\%/8.5\%$ for T04/PP04). Without correcting for the effect of AGN activity, the SN II host fibers (with similar host offset) are significantly less metal-rich than that of SN Ic host fibers.

Median offset differences between the SDSS fiber and SN location in right panel (in kpc): SN Ib (1.02), SN Ic (1.32), SN Ic-BL (1.56), SN II (1.11), SN IIb (1.66).

6.4. Host Specific Star Formation Rate from Fiber Spectra

SDSS spectra provide an estimate of the specific SFR ($\text{SFR } M_{\odot}^{-1} \text{ yr}^{-1}$) within the aperture of the fiber, which generally targets the host galaxy within the g' -band half-light radius. As can be seen in Figure 5, there is a progression of increasing specific SFR from SN II to SN Ib to SN Ic host spectra. SN Ic-BL host spectra also have significantly greater specific SFR than SN II host spectra.

Using visual inspection, we identified fibers that target the nuclei of host galaxies (to $z < 0.02$). These spectra yield significant evidence that the nuclei of SN (Ib+Ic) host galaxies have greater specific star formation rates than those of SN II host galaxies ($p=3.5\%$). This strong central star formation among SN (Ib+Ic) hosts may overwhelm AGN-patterned emission, explaining the relatively low AGN fraction among SN (Ib+Ic) host galaxies.

6.5. Extinction Inferred from Spectra

Although SN Ic hosts have stronger specific SFR within the half-light radius, the region where most SN Ic explode, the sites of SN Ic are not bluer than those of SN II (see Figure 2). Figure 6 shows that the high extinction of SN (Ib+Ic) host galaxies, measured from host spectra, may redden ongoing star formation in SN Ic host galaxies.

The host galaxies of SN IIb have less extinction than SN (Ib+Ic) host galaxies. The average extinction difference between SN (Ib+Ic) and SN IIb hosts is $A_V \sim 0.5$ mag, a $u'-z'$ reddening of ~ 0.6 mag. The approximately

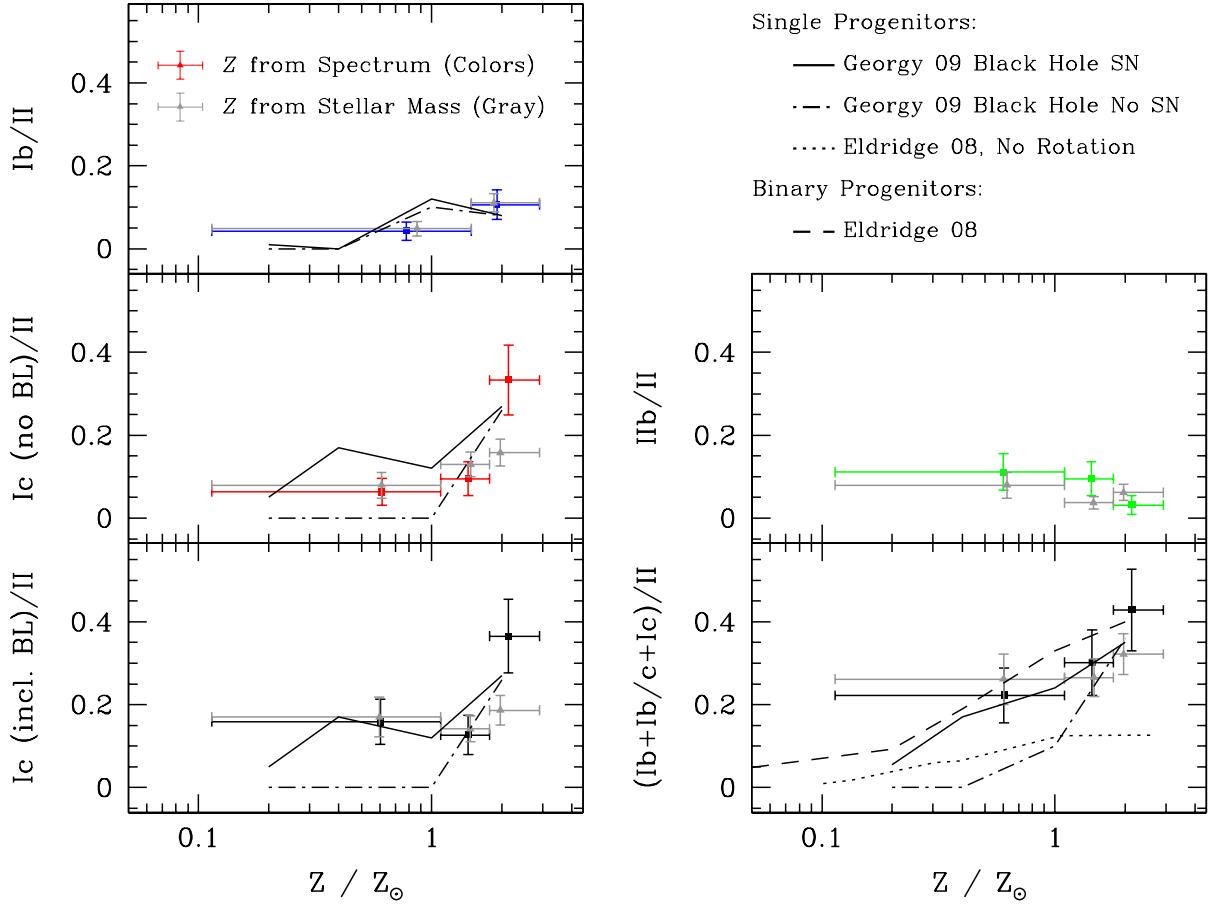


FIG. 7.— Ratio of stripped-envelope SN to SN II versus oxygen abundance (T04 calibration). The comparatively high fraction of SN ($Ib+Ib/c+Ic$) to SN II at subsolar metallicity in the right lower panel favors contributions from a binary progenitor population or explosions even after collapse to a black hole. Color points correspond to spectroscopic metallicity measurements, and gray points correspond to metallicities estimated from stellar masses using the Tremonti et al. 2004 mass-metallicity relation. The comparatively high fraction of SN II host fiber spectra with contamination from AGN activity (present only in massive, metal-rich galaxies) excludes a considerable fraction of metal-rich SN II host galaxies, inflating the apparent fraction of stripped-envelope SN in metal-rich galaxies (color points). Indeed, the stripped-envelope fraction is smaller using metallicities estimated from host galaxy stellar masses (gray) which do not suffer from an AGN selection effect. Dashed line is Eldridge et al. 2008 prediction for binary progenitors; dotted line is Eldridge et al. 2008 prediction for non-rotating single progenitors; and solid and dash-dot lines are Georgy et al. 2009 predictions for single, rotating progenitors (where a minimum helium envelope of $0.6 M_{\odot}$ separates SN Ib from SN Ic progenitors). Whether core collapse to a black hole can yield a SN explosion is not clear (e.g., Fryer et al. 1999), especially if high angular momentum does not support an accretion disk (Woosley et al. 1993). The Georgy et al. 2009 solid line prediction is where core collapse to a black hole produces SN while the dashed-line prediction is where core collapse to a black hole yields no SN. Vertical error bars reflect Poisson statistics while horizontal bars reflect the range of metallicities in each bin with the position of the vertical bar corresponding to the mean Z in the bin. Here $Z_{\odot} = 8.86$ from Delahaye et al. 2010.

similar internal extinctions of SN II and SN IIb hosts, however, suggest that the stellar populations near SN IIb likely are intrinsically bluer than those near SN II sites.

SN ($Ib+Ic$) host reddening is consistent ($p=38\%$) with that estimated along the line-of-sight to 19 SN ($Ib+Ic$) from their light curve colors by Drout et al. 2010 using an empirical model of SN Ib/c photometric color evolution. Comparison between the Drout et al. 2010 sample and the SN II host A_V distribution yields $p=13\%$. Here we plot only the Drout et al. 2010 Gold and Silver SN. There is a median $A_V \sim 1.2$ mag extinction through SN ($Ib+Ic$) host fiber apertures ($E(B-V) \sim 0.4$ mag).

7. RELATIVE FREQUENCIES OF CORE-COLLAPSE SN AS A FUNCTION OF METALLICITY

Figure 7 plots the ratio of stripped-envelope SN (including SN IIb) to SN II with increasing host galaxy oxygen abundance. Vertical error bars show the Poisson

uncertainties, while horizontal bars indicate the range of metallicities in each bin. The color points are calculated from successful *spectroscopic* metallicity measurements, while the gray points are estimated using *stellar mass* as a metallicity proxy, applying the Tremonti et al. 2004 mass-metallicity relation.

AGN emission, present disproportionately in SN II host spectra, is found primarily in high-mass, high-metallicity galaxies. This selection effect misleadingly *inflates* the apparent ratio SN ($Ib+Ic$) / SN II (color points) in the highest metallicity bin. Indeed, the ratio at high metallicity calculated instead using stellar masses as a proxy (which has no similar selection effect) is significantly lower (gray points). Earlier efforts using SDSS fiber spectra (i.e., Prieto et al. 2008), which also exclude AGN-contaminated spectra, have not noted this strong selection effect at high metallicity.

We compare relative rates to the model predictions for single, rotating progenitors (Georgy et al. 2009),

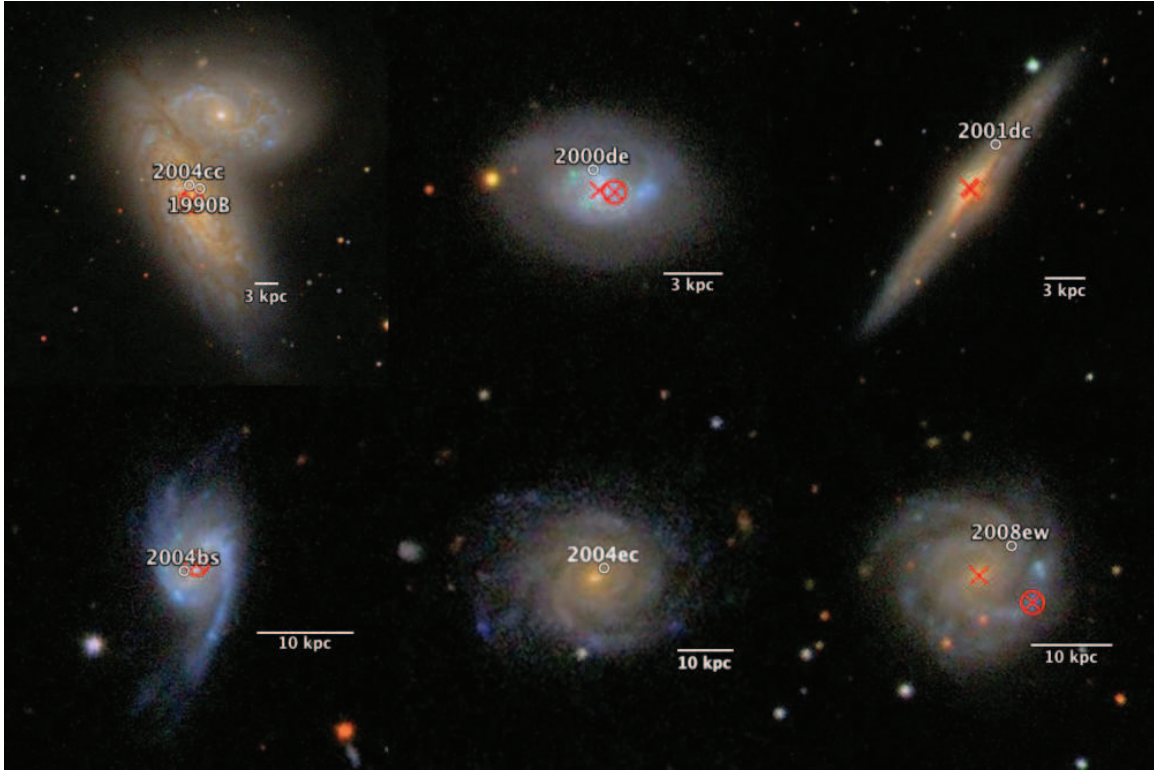


FIG. 8.— SDSS color composite images of 6 SN Ib, SN Ic, and SN II host galaxies in our sample. These include: SN 1990B (Ic), SN 2004cc (Ic), SN 2000de (Ib), SN 2001dc (IIP), SN 2004bs (Ib), SN 2004ec (IIn), and SN 2008ew (Ic). Red cross hatches show SDSS fibers positions yielding oxygen abundance measurements. An additional red circle marks fibers whose host offsets are within 3 kpc of the SN offset.

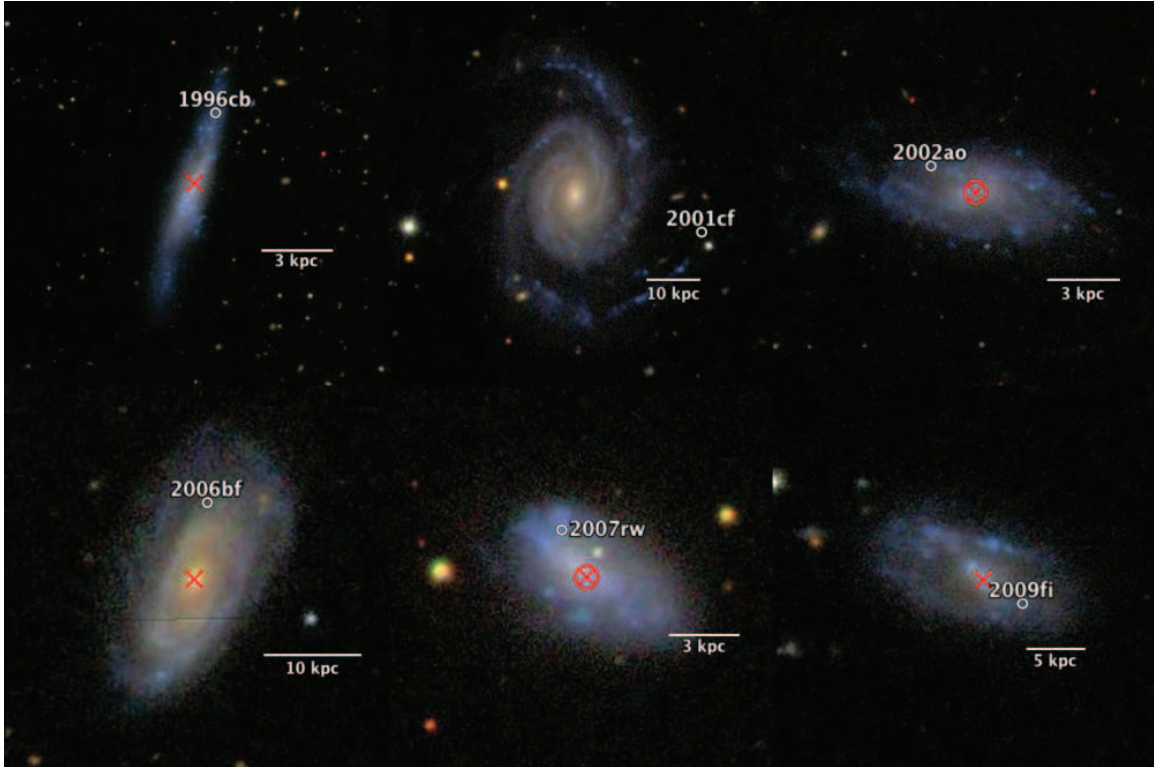


FIG. 9.— SDSS color composite images of 6 SN IIb in our sample. Their local environments are substantially bluer than those of SN Ib, SN Ic, and SN II. Red cross hatches show SDSS fibers positions yielding oxygen abundance measurements. An additional red circle marks fibers whose host offsets are within 3 kpc of the SN offset.

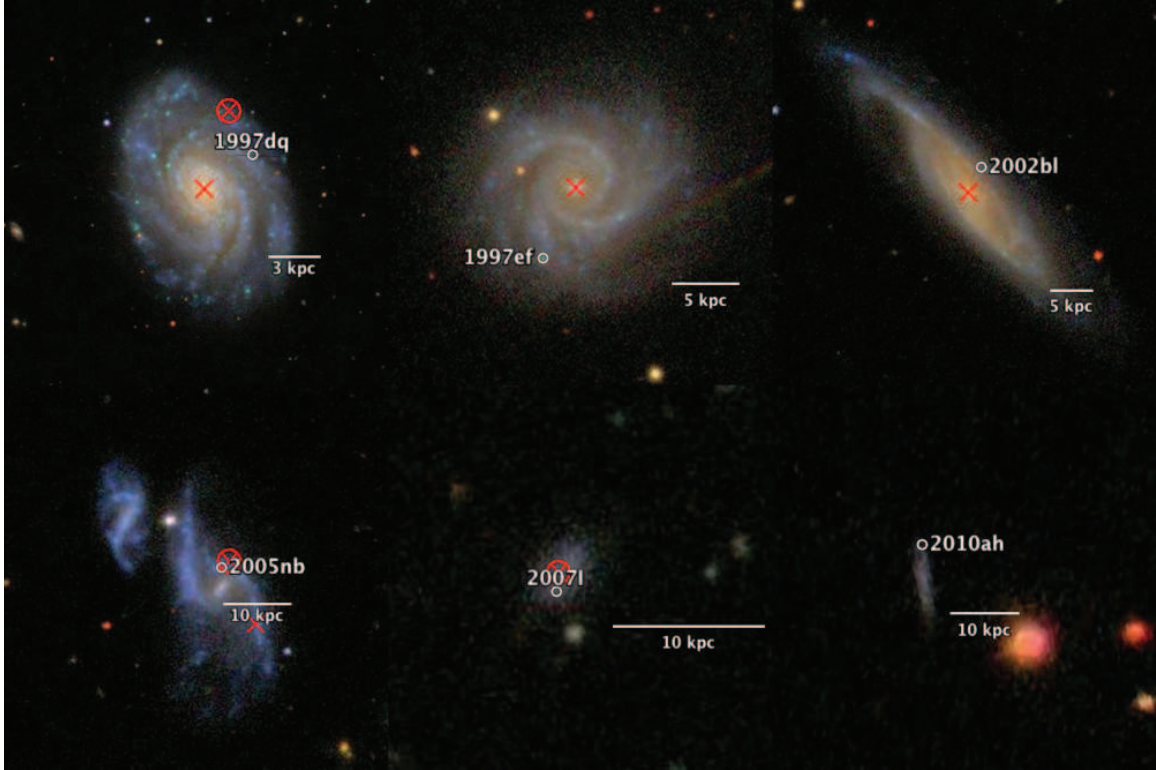


FIG. 10.— SDSS color composite images of 6 SN Ic-BL in our sample. SN Ic-BL in our sample occurred preferentially in lower-mass, low-metallicity host galaxies. Red cross hatches show SDSS fibers positions yielding oxygen abundance measurements. An additional red circle marks fibers whose host offsets are within 3 kpc of the SN offset.

single, non-rotating progenitors (Eldridge et al. 2008), and binary progenitors (Eldridge et al. 2008). Plotted Georgy et al. 2009 predictions were made with the assumption that a minimum helium envelope of $0.6 M_{\odot}$ separates the progenitors of SN Ib and SN Ic. Because core collapse to a black hole may not yield a SN explosion (e.g., Fryer et al. 1999), especially if high angular momentum does not support an accretion disk (Woosley et al. 1993), Georgy et al. 2009 calculated predictions where viable SN occur after core collapse to (a) only neutron stars and (b) neutron stars and black holes. These predictions adopted $2.7 M_{\odot}$ as the maximum mass of neutron star (Shapiro & Teukolsky 1983) and use the Hirschi et al. 2005 relation between neutron star mass and the mass of the carbon-oxygen core.

Model predictions are parameterized by Z/Z_{\odot} , requiring us to subtract the solar value from $12+\log(\text{O}/\text{H})$ estimates for each host galaxy to compute $\log(Z/Z_{\odot})$. The value of the solar metallicity is, however, not well constrained. Atmospheric modeling favors lower solar values (e.g., $12+\log(\text{O}/\text{H})=8.69$; Asplund et al. 2009) than helioseismic analyses (e.g., $12+\log(\text{O}/\text{H})=8.86$; Delahaye et al. 2010). Here we use the helioseismic value of Delahaye et al. 2010.

Returning to our data, we note that the spectroscopic oxygen abundance measurements should, on average, be *overestimates* of the oxygen abundance at the SN site because the SDSS fibers are concentrated toward the inner regions of the galaxies. Likewise, abundances calculated from host masses and the Tremonti et al. 2004 $M-Z$ relation should also be overestimates, because the Tremonti et al. 2004 relation is a fit to SDSS stellar masses and fiber metallicities.

The models for binary progenitors (Paczynski 1967; Podsiadlowski et al. 1992; Eldridge et al. 2008; Yoon et al. 2010; Claeys et al. 2011) in Figure 7 predict a higher fraction of stripped-envelope SN at low metallicities than do the single progenitor models (where core-collapse to a black hole does not yield a SN). This is because binary interaction can effectively strip away the outer envelopes of progenitors at low metallicities where wind-driven mass loss is not strong enough to expel the outer envelopes of most single massive stars (Eldridge et al. 2008; Smartt 2009; Yoon et al. 2010). Low metallicity stars that do lose their envelopes to winds have such large mass that their cores will collapse to a black hole. Given these model predictions, the comparatively high fraction of SN (Ib+Ib/c+Ic) to SN II at subsolar metallicity in the right lower panel favors contributions from a binary progenitor population or SN that accompany collapse to a black hole.

Smith et al. 2010b note that single star models use constant rates of wind-driven mass loss substantially greater than those observed, although episodic mass loss may speed loss of the outer envelopes. Lower wind-loss rates would imply a diminished fraction of single progenitors.

Splitting our sample in two at $z = 0.015$, the same trends persist in both the low and high redshift subsamples, indicating that they do not result from luminosity-dependent selection effects.

8. TESTS AND POTENTIAL SYSTEMATIC EFFECTS

8.1. Fiber Aperture Coverage

SDSS spectroscopic fiber apertures have a fixed radius of $1.5''$. At increasing redshift, this aperture radius corresponds to larger physical scales: 0.3 kpc at $z=0.01$; 0.6 kpc at $z=0.02$; and 1.17 kpc at $z=0.04$. For a sample of 11 NGC spiral galaxies, van Zee et al. 1998 found a mean radial abundance gradient of $-0.052 \text{ dex kpc}^{-1}$. While metallicity gradients vary among galaxies and have some dependence on, for example, host galaxy morphology (e.g., Kewley et al. 2006) and the metallicity calibration (e.g., Moustakas et al. 2010), we use this as a representative value.

Within the targeted sample ($z < 0.023$), nuclear spectroscopic fibers extend at most 0.68 kpc away from the host center, corresponding to systematic shifts of order only $\sim 0.025 \text{ dex}$. Galaxy-impartial SN discoveries (to $z < 0.08$) account for a significant fraction of only the SN Ic-BL sample. The difference between the median abundances for SN Ic-BL and SN Ic hosts is $\sim 0.5 \text{ dex}$, substantially greater than an aperture effect may yield.

8.2. Classification

There may be variation among the classification practices of the different surveys that contribute to our samples. A concern is that surveys that monitor different host galaxy populations (e.g., galaxy-impartial and targeted) could have different classification practices, such as use of automated classification tools (e.g., SNID (Blondin & Tonry 2007)) or multi-epoch spectroscopic follow up. For instance, the helium lines that identify SN Ib often emerge only after a couple of weeks (e.g., Li et al. 2011b).

8.3. Fiber Targeting

The SDSS object detection algorithm mistakenly split many galaxies of large angular size into two or more components [see Fig. 9 of Blanton et al. 2005]. The SDSS targeting algorithm then placed fibers on these false components, sometimes at significant offset from the true galaxy center. The error rate of these algorithms could depend on galaxy morphology (e.g., irregularity or an interacting neighbor), and we checked whether the offsets of fiber measurements depend on SN type. However, we found no evidence of strong variation with SN type.

SDSS fibers often target the local maxima of galaxy light distributions, including host nuclei and bright HII regions. In our sample, fibers have mean offset of $0.45 \times r_{\text{half-light}}$, while matched fibers (where $|r_{\text{env}} - r_{\text{fiber}}| < 3 \text{ kpc}$) have mean offset of $0.55 \times r_{\text{half-light}}$. Therefore, fiber sites are highly likely to be more metal-rich on average than they would be if SDSS fibers sampled galaxy light distributions more democratically. However, the fibers' offset distribution does not vary strongly with SN type.

The lifetimes of HII regions may be shorter than the those of the progenitors (private communication; N. Smith), and the signal at the SN site may be too weak. Programs that take host spectra at the location of the SN (e.g., Anderson et al. 2010; Modjaz et al. 2011; Leloudas et al. 2011) may only extract a metallicity estimate when there is sufficient nebular emission through the slit. Any such S/N requirement could possibly act as a type-dependent selection effect. The SDSS targets bright nuclei or HII regions, moderating any such effect in our analysis.

9. DISCUSSION

Our study of core-collapse host environments has revealed several statistically significant patterns. We have found that the u' - z' colors of SN I Ib and SN Ic-BL (without an associated LGRB) environments are blue in comparison to those of other stripped-envelope SN environments. The host specific SFR ($\text{SFR } M_{\odot}^{-1} \text{ yr}^{-1}$) is higher, on average, for types whose SN spectra indicate more complete loss of the progenitor's outer envelopes (i.e., SN Ib, SN Ic, SN Ic-BL). Spectroscopy also shows that SN Ic-BL host galaxies are more metal-poor than the hosts of normal SN Ic explosions, while SN I Ib hosts also are more metal-poor and have less extinction, on average, than SN Ib or SN Ic host galaxies.

A surprising effect is that spectroscopic contamination by AGN is higher among SN II hosts than SN (Ib+Ic) hosts. This is important to the correct interpretation of host galaxy properties from SDSS spectroscopy.

This study is statistical, and we have shown only that samples are drawn from differing underlying distributions in our comparisons. The distinctions we present are consistent with even considerable variation among the environments of individual examples of each SN type.

9.1. *Synthesizing Patterns*

There are strong connections among the type-dependent patterns in host galaxy photometry and spectroscopy:

- Host galaxies of SN Ic-BL generally have low mass and high specific SFR, helping to explain the blue colors at broad-lined SN Ic explosion sites. SN I Ib typically are found beyond the g' -band half-light radius in massive hosts, offering explanation for the blue colors of their sites. SN Ic-BL and SN I Ib host galaxies have lower abundances than SN Ic and SN Ib hosts, respectively.
- SN Ic often erupt at small offsets in massive galaxies with strong specific SFR, high oxygen abundance, and high extinction measured from fiber spectra. These fibers generally collect light from within the host's g' -band half-light radius. These explosion sites help to explain the high surface brightnesses near SN Ic explosion sites. High interstellar reddening helps to explain why the colors near SN Ic sites have colors similar to those of SN II, despite their hosts' high specific SFR.

The u' - z' color and u' surface brightness near SN explosion sites considerably separate SN I Ib, SN Ic, and SN Ic (see Figure 2). SN Ic sites predominantly have high surface brightness, while SN I Ib populate lower-surface brightness but extremely blue environments. SN Ib largely occupy the parameter space between the SN I Ib and the SN Ib. By contrast, however, the explosion sites of SN II have no specific locus in the color-brightness plane.

These patterns suggest that the fraction of stripped-envelope SN to Type II SN may not vary strongly with environment. Perhaps the stars that may explode as SN I Ib for one value of mass or metallicity instead explode as SN Ib or SN Ic in other environments where the chemistry, for example, is different.

9.2. *SN Ib, SN I Ib, and SN II Environments*

The best-studied example of a Type I Ib, SN 1993J, exploded at a distance of only 3.6 Mpc in M81 (Filippenko et al. 1993; Matheson et al. 2000), and archival imaging revealed that its progenitor was a K-type supergiant (Aldering et al. 1994). HST imaging after the SN disappeared found evidence for a B-type supergiant binary companion (Van Dyk et al. 2002; Maund et al. 2004). More recent studies of the sites of other SN I Ib suggest, however, that a fraction of the SN I Ib population may erupt from massive single stars (e.g., Crockett et al. 2008). Chevalier & Soderberg 2010 analyzed the radio emission, optical shock breakout, and nebular emission of a sample of SN I Ib to constrain the extent of their progenitors' envelopes and the properties of their circumstellar material. They favor two progenitor populations: (a) extended progenitors (SN 1993J, SN 2001gd) with hydrogen envelope mass greater than $\sim 0.1 M_{\odot}$ and slow, dense winds and (b) more compact and massive Wolf-Rayet progenitors (SN 1996cb, SN 2001ig, SN 2003bg, SN 2008ax, and SN 2008bo) with a less massive hydrogen envelope and lower density winds. PTF11eon/SN 2011dh, a SN I Ib (Arcavi et al. 2011; Marion et al. 2011), was recently discovered by amateur astronomer Amadee Riou in M51, where pre-explosion HST imaging exists of the SN site. Analysis of the archival images finds evidence for a supergiant with $T_{\text{eff}} \sim 6000$ K at or near the SN site (Van Dyk et al. 2011; Maund et al. 2011). Radio and X-ray observations (Soderberg et al. 2011) and the optical spectroscopic and photometric evolution (Arcavi et al. 2011) both favor a compact progenitor, however, suggesting that this star may be a binary companion or not associated with the SN.

Our analysis finds three statistically significant, plausibly related patterns in the host environments of SN I Ib: SN I Ib environments are bluer than the environments of SN Ib, SN Ic, and SN II; their host galaxies are more metal-poor than SN Ib or SN Ic hosts; and their host galaxy interstellar extinction is less than that of SN (Ib+Ic). These trends are statistically significant even when we analyze only the locations of targeted SN.

An unambiguous implication of the exceptionally blue colors of SN I Ib environments is that the Type I Ib progenitor population is distinct from that of Type Ib explosions. Lack of hydrogen features near maximum light in SN Ib spectra may reflect a more extensive loss of the progenitor's hydrogen envelope. Comparatively metal-poor SN I Ib host galaxies suggest that metals may play an important role in achieving this loss of the outer envelope.

The SN I Ib population may erupt from a combination of massive single stars and progenitors in close binary systems, so a possibility is that the blue colors of SN I Ib environments indicate higher binary fractions. Although the current examples of each class are few, future efforts may be able to draw distinctions between the environments of the compact and extended SN I Ib progenitors proposed by Chevalier & Soderberg 2010.

Li et al. 2011a recently reported that the hosts of SN I Ib detected by LOSS had greater K-band luminosities than SN II-P hosts (with $p=6.9\%$). Lower SN I Ib progenitor metallicities are consistent with the PTF's dimin-

ished fraction of SN Ib and SN Ic-BL in ‘giant,’ presumably metal-rich galaxies, than in ‘dwarf’ galaxies: 1 SN Ib, 3 SN Iib, and 2 SN Ic-BL, and 9 SN II in ‘dwarf’ galaxies, and 2 SN Ib, 2 SN Iib, 7 SN Ic, 1 SN Ic-BL and 42 SN II in ‘giant’ galaxies (Arcavi et al. 2010).

9.3. SN Ic-BL Environments

Type Ic-BL are the SN that have been associated with coincident long duration gamma-ray burst (LGRB) explosions (Galama et al. 1998; Matheson et al. 2003; Stanek et al. 2003; Hjorth et al. 2003; Modjaz et al. 2006; see Woosley & Bloom 2006 and Modjaz 2011 for reviews). Modjaz et al. 2008 showed that SN Ic-BL with associated LGRB prefer more metal-poor environments than do SN Ic-BL without an LGRB (but see Levesque et al. 2010).

We find that host galaxies of SN Ic-BL (without an associated LGRB) follow a significantly more metal-poor distribution than the hosts of normal SN Ic (or SN Ib) explosions, even when only galaxy-impartial discoveries are considered. The colors of SN Ic-BL local environments also follow a bluer distribution than those of SN Ic, further evidence for different progenitor populations. SN Ic-BL host galaxies have strong specific SFRs, similar to those of normal SN Ic.

Lower Type Ic-BL progenitor oxygen abundances may imply reduced rates of wind-driven mass loss, potentially enabling SN Ic-BL progenitor to retain greater angular momentum (e.g., Kudritzki 2002; Heger et al. 2003; Eldridge & Tout 2004; Vink & de Koter 2005). High angular momentum before the explosion may be important to the production of high velocity ejecta (Woosley et al. 1993; Thompson et al. 2004). Nonetheless, the means by which SN Ic-BL progenitors shed their outer envelopes, if not through their high metallicity, needs explanation and may involve Roche lobe overflow (Podsiadlowski et al. 1992; Nomoto et al. 1995), stellar mergers (Podsiadlowski et al. 2010), or perhaps deep mixing.

Here our measurements support a picture where both SN Ib and SN Ic have more metal-rich hosts on average than SN Ic-BL, consistent with the host galaxy magnitudes measured by Arcavi et al. 2010. It presents a contrast with the results of Modjaz et al. 2011 who recently measured the oxygen abundances at the *sites* of SN Ic-BL, SN (Ib+Iib), and SN Ic. There the SN Ic-BL distribution falls intermediate between those of SN (Ib+Iib) and SN Ic, although it is more similar to the comparatively metal-poor SN (Ib+Iib) distribution and neither comparison is statistically significant. These contrasting trends may relate to fact that Modjaz et al. 2011 constructed their samples for each SN type from equal numbers of galaxy-impartial and targeted SN discoveries, or the inclusion of SN Iib (which we find inhabit metal-poor environments) with SN Ib. Modjaz et al. 2011 measurements were also taken at the explosion site, which may often differ significantly from the host abundance measured from SDSS fiber spectra (0.13 dex average disagreement with *nuclear* fiber measurements).

Svensson et al. 2010 found that host galaxies of LGRBs had smaller star masses than core-collapse SN hosts and had high surface brightness and more massive stellar populations. The only SN-LGRB that met our sample criteria, SN 2006aj, has low host stellar mass and

comparatively blue $u'-z'$ color near the explosion site.

9.4. SN Ib, SN Ic, and SN II Environments

In an earlier paper (Kelly et al. 2008), we showed that, while the positions of the other core-collapse SN follow the distribution of their hosts’ light, Type Ic SN trace the brightest regions of their host galaxies in a pattern similar to that followed by LGRB (Fruchter et al. 2006). Possible explanations for this pattern include shorter lifetimes and higher masses of SN Ic progenitors (Raskin et al. 2008; Leloudas et al. 2010; Eldridge et al. 2011) as well as preference for metal-rich regions near the centers of hosts. Anderson & James 2008 showed, subsequently, that SN Ic also track their hosts’ $H\alpha$ emission more closely than SN II (their comparison with SN Ib lacked statistical significance).

The SDSS fiber spectra of core-collapse host galaxies, which generally sample inside of the g' -band half-light radius, reveal an increasing progression of specific SFR from SN II to SN Ib to SN Ic (and SN Ic-BL) hosts. This pattern persists when we study only the spectra from fibers targeting the host nucleus. SN Ic explode at comparatively small host offset, linking them to the strong star formation near their hosts’ centers.

We find that the central star formation that yields SN Ic generally has high chemical abundance and extinction from interstellar dust. A SN Ic progenitor population tracking high metallicity would be expected to explode in massive galaxies with strong star formation in metal-rich gas near their centers, the pattern we observe.

The colors of SN Ib and SN Ic explosion sites may offer evidence that their progenitors are also younger and more massive than the progenitors of SN II. The distribution of the apparent $u'-z'$ color at SN Ib and SN Ic sites is similar to that at SN II sites. However, we find that SN (Ib+Ic) host galaxies have higher interstellar extinction ($\Delta A_V \sim 0.5$ mag). This suggests that SN (Ib+Ic) sites have intrinsically bluer color than SN II sites, perhaps indicative of younger progenitor stellar populations.

SN Ib explosion sites have higher u' -band surface brightnesses than SN II sites, while SN Ib host galaxies generally have lower abundance than SN Ic in our sample. There is no statistically significant difference between the SN Ib and SN Ic host offset distributions in our sample ($p=75\%$), which may imply that host offset cannot, on its own, explain the uniquely strong association of SN Ic with bright host galaxy pixels (Kelly et al. 2008).

While analyses of pre- and post-explosion imaging have not yet identified a progenitor of a SN Ib or SN Ic, red supergiants have been found at the sites of SN II-P explosions (e.g., Barth et al. 1996; Van Dyk et al. 1999, 2003b, 2003a, 2010; Smartt et al. 2001, 2003, 2004; Li et al. 2005, 2007; Maund & Smartt 2005). Smartt et al. 2009 favor a 8.5-16.5 M_\odot mass range for SN II progenitors, although extinction along the line of sight to the progenitors is not well constrained (e.g., Walmswell & Eldridge 2011). Smith et al. 2010b note that Wolf Rayet stars in binary systems, possible progenitors of SN Ib and SN Ic, are expected to be less luminous than single Wolf Rayet stars. Brighter companions may outshine Wolf Rayet progenitors, although mass-gaining companions may, in some cases, explode first (Podsiadlowski et al. 1992; Eldridge et al. 2011). Even

for progenitors with close binary companions, metallicity and mass are expected to be important in determining the composition of the outer envelope, even though substantial mass loss may occur through Roche lobe overflow (Smith et al. 2010b; Yoon et al. 2010; Eldridge et al. 2011).

Prantzos & Boissier 2003 and Boissier & Prantzos 2009 found that SN (Ib+Ib/c+Ic) hosts have greater absolute M_B luminosities than SN II hosts. Prieto et al. 2008 previously compared the T04 metallicities of SN (Ib+Ic) and SN II host galaxies available in the SDSS DR4, finding $p=5\%$ evidence for a difference (they did not make note of the effect of AGN contamination). Van den Bergh 1997, Tsvetkov et al. 2004, Hakobyan et al. 2009, Anderson & James 2009, and Leaman et al. 2011 have found that SN (Ib+Ib/c+Ic) occur preferentially toward galaxy centers, where oxygen abundances are generally higher. Haberman et al. 2010 and Anderson et al. 2011, in a study of SN sites in Arp 299, have explored explanations for these patterns.

Modjaz et al. 2011 find a significant difference (~ 0.2 dex on average) between the oxygen abundances at the sites of 12 SN Ic and a mixed sample of 16 SN (Ib+Iib) for one of three oxygen abundance calibrations (although see Anderson et al. 2010 and Leloudas et al. 2011). When only abundances measured at the SN site from these three studies are compared, a significant difference between SN Ib and SN Ic metallicities computed with the Pettini & Pagel 2004 diagnostic is evident (M. Modjaz, private comm. and in prep.).

9.5. SN IIn Environments

Among our set of host measurements, we find no statistically significant differences between the characteristics of SN IIn host environments and those of normal SN II.

Narrow line emission characterizes SN IIn spectra (Schlegel 1990) and is thought to be the result of the interaction of the ejecta with high density surrounding material. The existence of dense circumstellar material likely indicates strong pre-explosion mass loss (e.g., Chugai & Danziger 1994) and can increase the optical luminosity of the SN by thermalizing the emerging blast wave (e.g., Woosley et al. 2007; Smith et al. 2010a; van Marle et al. 2010).

Luminous Blue Variable (LBV) stars (e.g., η Car), with their high mass loss rates ($> 10^{-4} M_{\odot} \text{yr}^{-1}$), have been suggested as candidate progenitors, although standard stellar modeling positions the LBV period before an ultimate Wolf-Rayet phase (e.g., Langer 1993; Maeder et al. 2005). Dwarkadas 2011 has recently suggested that observations may only present a convincing case for an LBV progenitor in the case of SN 2005gl (Gal-Yam et al. 2007; Gal-Yam & Leonard 2009). Other means of potentially producing regions of high density circumstellar material include, for example, pulsation-driven superwinds from red supergiants (RSGs) (Yoon & Cantiello 2010).

Our data suggest that SN IIn progenitors may have a range of properties (including mass) similar to those that contribute to the Type II population. Anderson & James 2009, who have also studied SN IIn explosion sites, found no significant difference between the mean radial offsets of 12 SN IIn and 35 SN IIP from the host galaxy center.

10. CONCLUSIONS

SN Iib and SN Ic-BL erupt in environments with exceptionally blue color. SN Iib sites often have large host offsets, while SN Ic-BL generally have comparatively low mass host galaxies. By contrast, SN Ib and especially SN Ic environments have less extreme colors, similar to those of SN II sites, but with exceptionally high u' -band surface brightness. SN Ib and SN Ic generally erupt from regions within the g' -band half-light radii of high stellar mass galaxies. The colors and surface brightnesses of SN II as well as SN IIn environments show no strong distinguishing pattern.

The centers of SN Ic host galaxies are generally dusty, metal-rich, and have high specific SFR. Stronger interstellar extinction associated with SN Ic sites may explain why they are not bluer than SN II sites, despite higher specific SFR. The central regions of SN Ib host galaxies are less metal-rich and have smaller specific SFR than those of SN Ic hosts.

We find that SN Iib host galaxy spectra are more metal-poor than SN Ib host galaxy spectra, statistically significant even among only targeted SN discoveries. SN Ic-BL host galaxies are also less metal-rich than SN Ic host galaxies, even among only galaxy-impartial discoveries.

The specific SFR measured from fiber spectra is higher, on average, for types whose SN spectra indicate more complete loss of the progenitor's outer envelopes (e.g., SN Ic, SN Ic-BL). Even among only spectra of galaxy nuclei, SN (Ib+Ic) host spectra have stronger specific SFR than SN II host spectra.

The non-negligible fraction of stripped-envelope SN in low-metallicity host galaxies may indicate that some stripped-envelope SN have binary progenitors or, alternatively, single progenitors that collapse to a black hole.

Drout et al. 2010 have estimated the line-of-sight extinction instead inferred from the colors of SN light curves. The interstellar reddening we find from SDSS fiber spectra of SN Ib and SN Ic hosts yield consistent values of A_V .

AGN emission, which makes spectra unusable for abundance measurements and is found primarily in high-metallicity galaxies, leads us to exclude a larger fraction of SN II ($21 \pm 3\%$ (42/196)) than SN (Ib+Ic) host spectra ($9 \pm 4\%$ (4/47)). This produces an overestimate of SN (Ib+Ic) / SN II in high-metallicity environments from SDSS spectra alone. The ratio is lower when we use host stellar mass as an oxygen abundance proxy, impervious to AGN.

Stellar mass estimates, robust to AGN contamination, provide evidence that SN (Ib+Ic) / SN II increases in more massive, metal-rich galaxies, a trend that retains significance when we consider only targeted SN discoveries.

We find no strong difference between the environments of SN IIn and the normal SN II population.

Thanks especially to M. Modjaz for her perceptive comments and to D. Burke for help with both supporting observations and editorial feedback. We also thank P. Challis, H. Marion, N. Zakamska, S. Akiyama, S. Allen, R. Romani, S-C. Yoon, M. Blanton, N. Smith, A. von der Linden, M. Allen, and D. Applegate for their advice and help. We acknowledge the MPA-JHU collaboration for

making their catalog publicly available and Google Sky for help in producing color galaxy images. RPK's supernova research at the Center for Astrophysics is supported by NSF grant AST0907903.

Funding for the SDSS and SDSS-II has been provided by the Alfred P. Sloan Foundation, the Participating Institutions, the National Science Foundation, the U.S. Department of Energy, the National Aeronautics and Space Administration, the Japanese Monbukagakusho, the Max Planck Society, and the Higher Education Funding Council for England.

The SDSS is managed by the Astrophysical Research Consortium for the Participating Institutions. The Participating Institutions are the American Museum of Natural History, Astrophysical Institute Potsdam, Univer-

sity of Basel, Cambridge University, Case Western Reserve University, University of Chicago, Drexel University, Fermilab, the Institute for Advanced Study, the Japan Participation Group, Johns Hopkins University, the Joint Institute for Nuclear Astrophysics, the Kavli Institute for Particle Astrophysics and Cosmology, the Korean Scientist Group, the Chinese Academy of Sciences (LAMOST), Los Alamos National Laboratory, the Max-Planck-Institute for Astronomy (MPIA), the Max-Planck-Institute for Astrophysics (MPA), New Mexico State University, Ohio State University, University of Pittsburgh, University of Portsmouth, Princeton University, the United States Naval Observatory, and the University of Washington.

REFERENCES

- ????
08. 1
- Aldering, G. et al. 2002, in Presented at the Society of Photo-Optical Instrumentation Engineers (SPIE) Conference, Vol. 4836, Society of Photo-Optical Instrumentation Engineers (SPIE) Conference Series, ed. J. A. Tyson & S. Wolff, 61–72
- Aldering, G., Humphreys, R. M., & Richmond, M. 1994, *AJ*, 107, 662
- Aldering, G. et al. 2005, *The Astronomer's Telegram*, 451, 1
- Anderson, J. P., Covarrubias, R. A., James, P. A., Hamuy, M., & Haberman, S. M. 2010, *ArXiv e-prints*
- Anderson, J. P., Haberman, S. M., & James, P. A. 2011, *MNRAS*, 416, 567, 1105.2837
- Anderson, J. P., & James, P. A. 2008, *MNRAS*, 390, 1527
- . 2009, *MNRAS*, 399, 559
- Arcavi, I. et al. 2010, *ArXiv e-prints*
- . 2011, *ArXiv e-prints*, 1106.3551
- Asplund, M., Grevesse, N., Sauval, A. J., & Scott, P. 2009, *ARA&A*, 47, 481, 0909.0948
- Astier, P. et al. 2006, *A&A*, 447, 31
- Baldwin, J. A., Phillips, M. M., & Terlevich, R. 1981, *PASP*, 93, 5
- Barbon, R., Buondì, V., Cappellaro, E., & Turatto, M. 1999, *A&A*, 139, 531
- Barth, A. J., van Dyk, S. D., Filippenko, A. V., Leibundgut, B., & Richmond, M. W. 1996, *AJ*, 111, 2047
- Bertin, E., Mellier, Y., Radovich, M., Missonnier, G., Didelon, P., & Morin, B. 2002, in *Astronomical Society of the Pacific Conference Series*, Vol. 281, *Astronomical Data Analysis Software and Systems XI*, ed. D. A. Bohlender, D. Durand, & T. H. Handley, 228
- Blanton, M. R., & Roweis, S. 2007, *AJ*, 133, 734
- Blanton, M. R. et al. 2005, *AJ*, 129, 2562
- Blondin, S., & Tonry, J. L. 2007, *ApJ*, 666, 1024
- Boissier, S., & Prantzos, N. 2009, *A&A*, 503, 137
- Brinchmann, J., Charlot, S., White, S. D. M., Tremonti, C., Kauffmann, G., Heckman, T., & Brinkmann, J. 2004, *MNRAS*, 351, 1151
- Cardelli, J. A., Clayton, G. C., & Mathis, J. S. 1989, *ApJ*, 345, 245
- Charlot, S., & Longhetti, M. 2001, *MNRAS*, 323, 887
- Chevalier, R. A., & Soderberg, A. M. 2010, *ApJ*, 711, L40
- Chugai, N. N., & Danziger, I. J. 1994, *MNRAS*, 268, 173
- Claeys, J. S. W., de Mink, S. E., Pols, O. R., Eldridge, J. J., & Baes, M. 2011, *A&A*, 528, A131+, 1102.1732
- Crockett, R. M. et al. 2008, *MNRAS*, 391, L5
- Delahaye, F., Pinsonneault, M. H., Pinsonneault, L., & Zeppen, C. J. 2010, *ArXiv e-prints*, 1005.0423
- Dickinson, M., Giavalisco, M., & GOODS Team. 2003, in *The Mass of Galaxies at Low and High Redshift*, ed. R. Bender & A. Renzini, 324
- Dilday, B. et al. 2010, *ApJ*, 715, 1021
- Djorgovski, S. G. et al. 2008, *Astronomische Nachrichten*, 329, 263
- . 2011, *ArXiv e-prints*
- Drout, M. R. et al. 2010, *ArXiv e-prints*
- Dwarkadas, V. V. 2011, *MNRAS*, 23
- Eldridge, J. J., Izzard, R. G., & Tout, C. A. 2008, *MNRAS*, 384, 1109
- Eldridge, J. J., Langer, N., & Tout, C. A. 2011, *ArXiv e-prints*
- Eldridge, J. J., & Tout, C. A. 2004, *MNRAS*, 353, 87
- Filippenko, A. V. 1997, *ARA&A*, 35, 309
- Filippenko, A. V. 2003, in *From Twilight to Highlight: The Physics of Supernovae*, ed. W. Hillebrandt & B. Leibundgut, 171
- Filippenko, A. V., & Chornock, R. 2003, *IAU Circ.*, 8042, 4
- Filippenko, A. V., Matheson, T., & Ho, L. C. 1993, *ApJ*, 415, L103+
- Fioc, M., & Rocca-Volmerange, B. 1997, *A&A*, 326, 950
- . 1999, *ArXiv e-prints*
- Foley, R. J., Smith, N., Ganeshalingam, M., Li, W., Chornock, R., & Filippenko, A. V. 2007, *ApJ*, 657, L105
- Fruchter, A. S. et al. 2006, *Nature*, 441, 463
- Fryer, C. L., Woosley, S. E., & Hartmann, D. H. 1999, *ApJ*, 526, 152
- Gal-Yam, A., & Leonard, D. C. 2009, *Nature*, 458, 865
- Gal-Yam, A. et al. 2007, *ApJ*, 656, 372
- Galama, T. J. et al. 1998, *Nature*, 395, 670
- Georgy, C., Meynet, G., Walder, R., Folini, D., & Maeder, A. 2009, *A&A*, 502, 611
- Haberman, S. M., Anderson, J. P., & James, P. A. 2010, *ApJ*, 717, 342, 1005.0511
- Hakobyan, A. A., Mamon, G. A., Petrosian, A. R., Kunth, D., & Turatto, M. 2009, *A&A*, 508, 1259
- Hardin, D. et al. 2000, *A&A*, 362, 419
- Heger, A., Fryer, C. L., Woosley, S. E., Langer, N., & Hartmann, D. H. 2003, *ApJ*, 591, 288
- Hirschi, R., Meynet, G., & Maeder, A. 2005, *A&A*, 443, 581
- Hjorth, J. et al. 2003, *Nature*, 423, 847
- Kaiser, N. et al. 2010, in Presented at the Society of Photo-Optical Instrumentation Engineers (SPIE) Conference, Vol. 7733, *Society of Photo-Optical Instrumentation Engineers (SPIE) Conference Series*
- Kauffmann, G. et al. 2003, *MNRAS*, 346, 1055
- Kelly, P. L., Hicken, M., Burke, D. L., Mandel, K. S., & Kirshner, R. P. 2010, *ApJ*, 715, 743, 0912.0929
- Kelly, P. L., Kirshner, R. P., & Pahre, M. 2008, *ApJ*, 687, 1201
- Kewley, L. J., & Ellison, S. L. 2008, *ApJ*, 681, 1183
- Kewley, L. J., Geller, M. J., & Barton, E. J. 2006, *AJ*, 131, 2004
- Kron, R. G. 1980, *ApJS*, 43, 305
- Kudritzki, R. P. 2002, *ApJ*, 577, 389
- Langer, N. 1993, *Space Sci. Rev.*, 66, 365
- Law, N. M. et al. 2009, *PASP*, 121, 1395
- Leaman, J., Li, W., Chornock, R., & Filippenko, A. V. 2011, *MNRAS*, 412, 1419
- Leloudas, G. et al. 2011, *ArXiv e-prints*
- Leloudas, G., Sollerman, J., Levan, A. J., Fynbo, J. P. U., Malesani, D., & Maund, J. R. 2010, *ArXiv e-prints*
- Levesque, E. M., Kewley, L. J., Graham, J. F., & Fruchter, A. S. 2010, *ApJ*, 712, L26
- Li, W., Chornock, R., Leaman, J., Filippenko, A. V., Poznanski, D., Wang, X., Ganeshalingam, M., & Mannucci, F. 2011a, *MNRAS*, 412, 1473

- Li, W. et al. 2011b, *MNRAS*, 412, 1441
- Li, W., Van Dyk, S. D., Filippenko, A. V., & Cuillandre, J.-C. 2005, *PASP*, 117, 121, arXiv:astro-ph/0412487
- Li, W., Wang, X., Van Dyk, S. D., Cuillandre, J.-C., Foley, R. J., & Filippenko, A. V. 2007, *ApJ*, 661, 1013, arXiv:astro-ph/0701049
- Maeder, A., Meynet, G., & Hirschi, R. 2005, in *Astronomical Society of the Pacific Conference Series*, Vol. 336, *Cosmic Abundances as Records of Stellar Evolution and Nucleosynthesis*, ed. T. G. Barnes III & F. N. Bash, 79
- Marion, G. H. et al. 2011, *The Astronomer's Telegram*, 3435, 1
- Matheson, T., Filippenko, A. V., Ho, L. C., Barth, A. J., & Leonard, D. C. 2000, *AJ*, 120, 1499
- Matheson, T., Filippenko, A. V., Li, W., Leonard, D. C., & Shields, J. C. 2001, *AJ*, 121, 1648
- Matheson, T. et al. 2003, *ApJ*, 599, 394
- . 2008, *AJ*, 135, 1598
- Maund, J. R. et al. 2011, *ArXiv e-prints*, 1106.2565
- Maund, J. R., & Smartt, S. J. 2005, *MNRAS*, 360, 288, arXiv:astro-ph/0501323
- Maund, J. R. et al. 2006, *MNRAS*, 369, 390
- Maund, J. R., Smartt, S. J., Kudritzki, R. P., Podsiadlowski, P., & Gilmore, G. F. 2004, *Nature*, 427, 129
- Mazzali, P. A., Deng, J., Maeda, K., Nomoto, K., Filippenko, A. V., & Matheson, T. 2004, *ApJ*, 614, 858, arXiv:astro-ph/0409575
- Miknaitis, G. et al. 2007, *ApJ*, 666, 674
- Modjaz, M. 2011, *Astronomische Nachrichten*, 332, 434, 1105.5297
- Modjaz, M., Kewley, L., Bloom, J. S., Filippenko, A. V., Perley, D., & Silverman, J. M. 2011, *ApJ*, 731, L4+
- Modjaz, M. et al. 2008, *AJ*, 135, 1136
- . 2006, *ApJ*, 645, L21
- Moustakas, J., Kennicutt, Jr., R. C., Tremonti, C. A., Dale, D. A., Smith, J., & Calzetti, D. 2010, *ApJS*, 190, 233
- Nomoto, K. I., Iwamoto, K., & Suzuki, T. 1995, *Phys. Rep.*, 256, 173
- Osterbrock, D. E. 1989, *Astrophysics of gaseous nebulae and active galactic nuclei*, ed. Osterbrock, D. E.
- Paczynski, B. 1967, *Acta Astron.*, 17, 355
- Pastorello, A. et al. 2007, *Nature*, 447, 829
- Perlmutter, S. et al. 1999, *ApJ*, 517, 565
- Pettini, M., & Pagel, B. E. J. 2004, *MNRAS*, 348, L59
- Podsiadlowski, P., Ivanova, N., Justham, S., & Rappaport, S. 2010, *MNRAS*, 406, 840
- Podsiadlowski, P., Joss, P. C., & Hsu, J. J. L. 1992, *ApJ*, 391, 246
- Prantzos, N., & Boissier, S. 2003, *A&A*, 406, 259
- Pravdo, S. H. et al. 1999, *AJ*, 117, 1616
- Prieto, J. L., Stanek, K. Z., & Beacom, J. F. 2008, *ApJ*, 673, 999
- Quimby, R., Mondol, P., Hoefflich, P., Wheeler, J. C., & Gerardy, C. 2005a, *IAU Circ.*, 8503, 1
- Quimby, R. M., Castro, F., Gerardy, C. L., Hoefflich, P., Kannappan, S. J., Mondol, P., Sellers, M., & Wheeler, J. C. 2005b, in *Bulletin of the American Astronomical Society*, Vol. 37, *American Astronomical Society Meeting Abstracts*, 171.02
- Raskin, C., Scannapieco, E., Rhoads, J., & Della Valle, M. 2008, *ApJ*, 689, 358
- Riess, A. G. et al. 1998, *AJ*, 116, 1009
- Sako, M. et al. 2005, in *22nd Texas Symposium on Relativistic Astrophysics*, ed. P. Chen, E. Bloom, G. Madejski, & V. Patrosian, 415–420
- Schlegel, D. J., Finkbeiner, D. P., & Davis, M. 1998, *ApJ*, 500, 525
- Schlegel, E. M. 1990, *MNRAS*, 244, 269
- Shapiro, S. L., & Teukolsky, S. A. 1983, *Black holes, white dwarfs, and neutron stars: The physics of compact objects*
- Smartt, S. J. 2009, *ARA&A*, 47, 63
- Smartt, S. J., Eldridge, J. J., Crockett, R. M., & Maund, J. R. 2009, *MNRAS*, 395, 1409, 0809.0403
- Smartt, S. J., Gilmore, G. F., Trentham, N., Tout, C. A., & Frayn, C. M. 2001, *ApJ*, 556, L29, arXiv:astro-ph/0105453
- Smartt, S. J., Maund, J. R., Gilmore, G. F., Tout, C. A., Kilkenny, D., & Benetti, S. 2003, *MNRAS*, 343, 735, arXiv:astro-ph/0301324
- Smartt, S. J., Maund, J. R., Hendry, M. A., Tout, C. A., Gilmore, G. F., Mattila, S., & Benn, C. R. 2004, *Science*, 303, 499, arXiv:astro-ph/0401235
- Smith, N., Chornock, R., Silverman, J. M., Filippenko, A. V., & Foley, R. J. 2010a, *ApJ*, 709, 856
- Smith, N., Li, W., Filippenko, A. V., & Chornock, R. 2010b, *ArXiv e-prints*
- Soderberg, A. M. et al. 2011, *ArXiv e-prints*, 1107.1876
- Stanek, K. Z. et al. 2003, *ApJ*, 591, L17
- Strauss, M. A. et al. 2002, *AJ*, 124, 1810
- Svensson, K. M., Levan, A. J., Tanvir, N. R., Fruchter, A. S., & Strolger, L. 2010, *MNRAS*, 479
- Thompson, T. A., Chang, P., & Quataert, E. 2004, *ApJ*, 611, 380
- Tremonti, C. A. et al. 2004, *ApJ*, 613, 898
- Tsvetkov, D. Y., Pavlyuk, N. N., & Bartunov, O. S. 2004, *Astronomy Letters*, 30, 729
- van den Bergh, S. 1997, *AJ*, 113, 197
- van den Bergh, S., & Tammann, G. A. 1991, *ARA&A*, 29, 363
- Van Dyk, S. D. et al. 2010, *ArXiv e-prints*, 1011.5873
- Van Dyk, S. D., Garnavich, P. M., Filippenko, A. V., Höflich, P., Kirshner, R. P., Kurucz, R. L., & Challis, P. 2002, *PASP*, 114, 1322
- van Dyk, S. D., Hamuy, M., & Filippenko, A. V. 1996, *AJ*, 111, 2017
- Van Dyk, S. D. et al. 2011, *ArXiv e-prints*, 1106.2897
- Van Dyk, S. D., Li, W., & Filippenko, A. V. 2003a, *PASP*, 115, 448, arXiv:astro-ph/0301346
- . 2003b, *PASP*, 115, 1289, arXiv:astro-ph/0307226
- Van Dyk, S. D., Peng, C. Y., Barth, A. J., & Filippenko, A. V. 1999, *AJ*, 118, 2331, arXiv:astro-ph/9907252
- Van Dyk, S. D., Peng, C. Y., King, J. Y., Filippenko, A. V., Treffers, R. R., Li, W., & Richmond, M. W. 2000, *PASP*, 112, 1532
- van Marle, A. J., Smith, N., Owocki, S. P., & van Veelen, B. 2010, *MNRAS*, 407, 2305
- van Zee, L., Salzer, J. J., Haynes, M. P., O'Donoghue, A. A., & Balonek, T. J. 1998, *AJ*, 116, 2805
- Vink, J. S., & de Koter, A. 2005, *A&A*, 442, 587
- Walmswell, J. J., & Eldridge, J. J. 2011, *ArXiv e-prints*, 1109.4637
- Wittman, D. M. et al. 2002, in *Presented at the Society of Photo-Optical Instrumentation Engineers (SPIE) Conference*, Vol. 4836, *Society of Photo-Optical Instrumentation Engineers (SPIE) Conference Series*, ed. J. A. Tyson & S. Wolff, 73–82
- Wood-Vasey, W. M. et al. 2004, *New Astronomy Reviews*, 48, 637
- Woosley, S. E., Blinnikov, S., & Heger, A. 2007, *Nature*, 450, 390
- Woosley, S. E., & Bloom, J. S. 2006, *ARA&A*, 44, 507, arXiv:astro-ph/0609142
- Woosley, S. E., Langer, N., & Weaver, T. A. 1993, *ApJ*, 411, 823
- Yoon, S., & Cantiello, M. 2010, *ApJ*, 717, L62
- Yoon, S., Woosley, S. E., & Langer, N. 2010, *ArXiv e-prints*
- Yost, S. A. et al. 2006, *Astronomische Nachrichten*, 327, 803

TABLE 7
HOST GALAXY MEASUREMENTS

SN	Vel. (km s ⁻¹)	Type	Offset Norm.	SSFR	T04 (dex)	PP04 (dex)	A _V (mag)	u'-z' (local)	Discov. Method	Discoverer
PTF09axi	19200	II	0.63					1.56	I	PTF
PTF09bce	6900	II	0.95					2.47	I	PTF
PTF09cjg	5700	II	0.69	-12.09			0.00	2.62	I	PTF
PTF09cvi	9000	II	1.61					1.81	I	PTF
PTF09dra	23100	II	0.96	-10.33	8.98	8.71	1.03	1.57	I	PTF
PTF09ebq	7050	II	0.21					1.88	I	PTF
PTF09ecm	8550	II	0.76					2.82	I	PTF
PTF09fbf	6300	II	0.65	-7.82	8.73	8.24	0.50	1.76	I	PTF
PTF09fmk	18930	II	1.00					2.15	I	PTF
PTF09fqa	9000	II	0.49					1.60	I	PTF
PTF09hdo	14100	II	1.04					2.28	I	PTF
PTF09hgz	8400	II	0.56					3.04	I	PTF
PTF09iex	6000	II	0.66					1.27	I	PTF
PTF09ige	19200	II	1.31	-9.85	8.85	8.63	0.65	1.15	I	PTF
PTF09ism	8700	II	2.14	-10.19	8.84	8.61	0.12	2.41	I	PTF
PTF09sh	11310	II	1.25	-9.86	9.01	8.73	0.68	1.54	I	PTF
PTF09tm	10500	II	0.55					1.83	I	PTF
PTF09uj	19530	II	0.54	-10.14	8.83	8.63	1.16	1.74	I	PTF
PTF10bau	7800	II	0.80	-9.14	9.11	8.77	0.66	2.34	I	PTF
PTF10bgl	9000	II	0.83	-8.61	8.91	8.54	0.90	1.73	I	PTF
PTF10cd	13650	II	0.70					0.57	I	PTF
PTF10con	9900	II	0.17	-10.29	8.86	8.64	1.11	2.59	I	PTF
PTF10cqh	12300	II	1.32					1.83	I	PTF
PTF10cwx	21900	II	0.70					1.26	I	PTF
PTF10cxq	14100	II	0.39					1.65	I	PTF
PTF10cxc	10200	II	0.58	-9.84	9.05	8.78	1.33	2.28	I	PTF
PTF10czt	13500	II	1.63					0.63	I	PTF
PTF10dk	22200	II	0.66					1.40	I	PTF
PTF10hvj	15540	II	0.09	-10.17	8.84	8.61	0.62	1.61	I	PTF
1990ah	5236	II	0.67					1.21	T	Pollas
1991ao	4923	II	1.42					2.15	T	Pollas
1992I	3588	II	3.71					3.57	T	Buil
1992ad	1270	II	1.12					0.97	T	Evans
1993W	5400	II	0.71					1.97	T	Pollas
1993ad	5167	II	1.48					1.78	T	Pollas
1994P	1078	II	2.01					1.70	T	Sackett
1994ac	5311	II	0.29					1.45	T	McNaught
1995H	1419	II	0.66					1.20	T	Mueller
1995J	2972	II	1.58	-10.17	8.64	8.58	0.32	0.67	T	Johnson
1995V	1517	II	0.76	-8.42	9.11	8.80	1.03	1.77	T	Evans
1995Z	4748	II	0.96					2.45	T	Mueller
1995ab	5700	II	1.48					0.56	T	Pollas
1995ag	1483	II	0.53					1.61	T	Mueller
1995ah	4410	II	0.86	-9.57	8.27	8.25	0.32	1.13	T	Popescu et a..
1995ai	5264	II	1.44					1.54	T	Pollas
1996B	4252	II	0.60					2.34	T	Gabrijelcic
1996an	1414	II	0.77	-8.58	8.91	8.63	0.91	1.30	T	Aoki
1996bw	5412	II	1.50					1.90	T	BAO Supernov..
1996cc	2166	II	0.87					1.63	T	Sasaki
1997W	5412	II	1.55					1.69	T	Berlind, Gar..
1997aa	3645	II	1.95					1.08	T	BAO Supernov..
1997bn	4096	II	0.36					2.07	T	BAO Supernov..
1997bo	3605	II	0.80	-8.50	7.92	7.99	0.12	1.79	T	BAO Supernov..
1997co	6993	II	0.64	-11.72			1.35	2.49	T	BAO Supernov..
1997cx	1529	II	0.60					1.26	T	Schwartz
1997db	1483	II	0.92					0.97	T	Schwartz
1997dn	1331	II	1.36	-7.76	8.98	8.52	1.35	1.77	T	Boles
1997ds	2833	II	0.53					1.89	T	BAO Supernov..
1998R	2022	II	0.44	-9.86	8.97	8.69	1.16	2.57	T	Berlind, Car..
1998W	3566	II	1.02					1.88	T	Lick Observa..
1998Y	3810	II	0.73					1.24	T	Lick Observa..
1998ar	3665	II	1.39	-12.15			0.14	1.70	T	BAO Supernov..
1998bm	1448	II	0.96	-7.89	8.43	8.08	0.65	0.35	T	Lick Observa..
1998dn	388	II	2.04					1.91	T	Beijing Astr..
1999D	3033	II	1.79					1.80	T	BAO Supernov..
1999an	1501	II	0.35	-9.24	8.62	8.32	0.22	0.82	T	BAO Supernov..
1999ap	12000	II	0.47				0.51	1.57	I	Nearby Galax..
1999cd	4249	II	1.28	-8.50	8.99	8.65	1.12	1.51	T	Lick Observa..
1999dh	3247	II	0.96					1.17	T	Lick Observa..
1999et	4873	II	1.18					1.66	T	Cappellaro
1999ge	5649	II	0.49	-10.94			0.85	2.42	T	Lick Observa..
1999gg	4282	II	0.67					1.74	T	Boles
1999gk	2547	II	1.21	-10.78	9.05	8.76	0.57	1.21	T	Berlind
1999gl	5083	II	0.09					2.45	T	Boles
2000I	6639	II	0.70	-9.33	9.17	8.89	0.86	2.23	T	Puckett

TABLE 7 — *Continued*

SN	Vel. (km s ⁻¹)	Type	Offset Norm.	SSFR	T04 (dex)	PP04 (dex)	A _V (mag)	u'-z' (local)	Discov. Method	Discoverer
2000au	5900	II	1.45	-12.19			0.00	2.09	T	Puckett, Lan..
2000cb	1927	II	1.14					1.92	T	Lick Observa..
2000el	2907	II	0.29					2.46	T	Puckett, Geo..
2000ez	3272	II	0.87	-8.70	8.67	8.30	0.09	1.10	T	Armstrong
2000fe	4222	II	1.28	-10.57			3.08	2.50	T	Lick & Tena..
2001H	5251	II	0.24					2.16	T	Holmes
2001J	3924	II	1.00	-10.12	8.80	8.67	0.30	0.95	T	Lick & Tena..
2001K	3272	II	0.88					2.21	T	Beijing Astr..
2001Q	3724	II	1.04					1.07	T	Lick & Tena..
2001aa	6166	II	1.91	-10.55			1.27	2.49	T	Armstrong
2001ab	5066	II	0.95					2.28	T	Lick & Tena..
2001ae	6996	II	1.83	-9.42	9.22	8.88	1.38	0.45	T	Lick & Tena..
2001ax	6000	II	1.56					3.32	I	Schaefer, QU..
2001bk	12900	II	0.95					2.01	I	QUEST
2001cl	4905	II	1.33					2.30	T	Lick & Tena..
2001cm	3420	II	1.08	-11.67			1.77	2.39	T	Beijing Obse..
2001cx	4834	II	1.54					2.06	T	Lick & Tena..
2001cy	4693	II	0.37					2.67	T	Lick & Tena..
2001ee	4483	II	1.29					1.91	T	Armstrong
2001fb	9450	II	1.21	-9.30	8.61	8.38	1.13	2.02	I	Sloan Digita..
2001fc	5027	II	0.67					2.98	T	Puckett, Cox
2001ff	3977	II	0.32	-10.34	8.99	8.77	1.44	2.81	T	Lick & Tena..
2001hg	2569	II	1.41	-9.02	9.13	8.83	0.80	1.37	T	Puckett, Seh..
2002an	3870	II	1.56					1.68	T	Sano
2002aq	5150	II	2.96					2.71	T	LOTOSS
2002bh	5200	II	1.37					1.72	T	LOTOSS
2002bx	2265	II	2.02	-10.91			1.52	3.04	T	LOTOSS; Bole..
2002ca	3264	II	1.33	-9.74	9.05	8.83	0.98	2.26	T	Puckett, Ker..
2002ce	2012	II	0.67	-8.80	8.97	8.57	0.61	1.33	T	Arbour
2002ej	4859	II	0.91					2.15	T	Puckett, Ker..
2002em	4059	II	1.80					2.48	T	Armstrong
2002ew	8920	II	1.35	-9.64	8.72	8.56	0.47	1.40	I	NEAT/Wood-Va..
2002gd	2686	II	1.71					1.43	T	Klotz; Pucke..
2002hg	2877	II	0.95	-9.09	8.85	8.56	0.56	1.75	T	Boles
2002hj	7090	II	1.39					1.03	I	NEAT/Wood-Va..
2002hm	3494	II	0.86	-9.31	8.71	8.45	0.14	0.49	T	Boles
2002ig	23100	II	0.41					0.47	I	Sloan Digita..
2002in	22800	II	0.41	-9.95	8.37	8.39	0.50	2.01	I	Sloan Digita..
2002ip	23700	II	0.50					1.55	I	Sloan Digita..
2002iq	16800	II	0.42	-9.55	8.29	8.25	0.40	0.87	I	Sloan Digita..
2002jl	19200	II	0.03					1.82	I	NEAT/Wood-Va..
2003C	5246	II	0.91					1.63	T	Puckett, Cox
2003O	4930	II	1.54					1.90	T	Rich
2003bk	1262	II	0.28	-11.36			1.87	3.62	T	LOTOSS
2003bl	4295	II	1.13	-8.98	9.26	8.89	2.07	2.35	T	LOTOSS
2003cn	5399	II	2.15	-10.06	9.09	8.81	0.67	0.53	T	LOTOSS
2003da	4152	II	0.59	-10.16	8.86	8.64	1.45	2.12	T	Boles
2003dq	13800	II	0.40					0.00	I	NEAT/Wood-Va..
2003ej	5131	II	1.46	-10.48	8.95	8.75	0.99	0.85	T	LOTOSS
2003hg	4298	II	0.29					3.04	T	LOTOSS
2003hk	6980	II	0.70					2.42	T	Boles; LOTOS..
2003hl	2454	II	0.52					2.67	T	LOTOSS
2003iq	2454	II	1.09					2.65	T	Llapasset
2003jc	5768	II	1.82					0.00	T	Lick Observa..
2003kx	1860	II	0.53					2.55	T	Armstrong
2003ld	4156	II	0.24	-8.73	8.78	8.44	0.83	1.95	T	Puckett, Cox
2003lp	2545	II	0.97					1.56	T	Puckett, Tot..
2004D	6184	II	0.85	-10.39	9.08	8.77	1.14	1.85	T	Lick Observa..
2004G	1583	II	1.30	-9.03	8.71	8.42	0.00	1.31	T	Kushida
2004T	6436	II	0.93	-11.28			0.21	2.30	T	Lick Observa..
2004Z	6933	II	1.20					2.09	T	Boles
2004bn	6659	II	1.10	-10.00	9.17	8.82	1.12	1.65	T	Lick Observa..
2004ci	4130	II	0.93	-8.43	9.17	8.86	2.27	2.29	T	Lick Observa..
2004dh	5820	II	0.77					2.69	T	Lick Observa..
2004ei	5755	II	0.09					3.13	T	Boles
2004ek	5228	II	175.81					2.08	T	Boles; Pucke..
2004em	4486	II	1.54					2.39	T	Armstrong
2004er	4411	II	1.48					1.25	T	Lick Observa..
2004gy	8070	II	1.16					1.70	I	Quimby et al.
2004ht	20100	II	1.28	-10.32			1.39	2.12	I	Frieman, SDS..
2004hv	18300	II	1.47					0.65	I	Frieman, SDS..
2004hx	4200	II	2.17					0.97	I	Frieman, SDS..
2004hy	17400	II	1.44	-10.15	8.69	8.55	0.40	1.76	I	Frieman, SDS..
2005H	3841	II	0.72	-9.06	9.11	8.74	1.23	2.06	T	Lick Observa..
2005I	5452	II	0.90					2.85	T	Lick Observa..

TABLE 7 — *Continued*

SN	Vel. (km s ⁻¹)	Type	Offset Norm.	SSFR	T04 (dex)	PP04 (dex)	A _V (mag)	u'-z' (local)	Discov. Method	Discoverer
2005Y	4920	II	0.56	-9.83	8.82	8.61	0.84	1.62	T	Lick Observa..
2005Z	5766	II	0.59	-9.75	9.26	8.79	1.98	2.65	T	Trondal, Sch..
2005aa	6403	II	0.93					2.65	T	Lick Observa..
2005ab	4624	II	1.14	-9.70	9.11	8.79	2.35	1.43	T	Itagaki
2005au	5449	II	0.76	-8.86	8.92	8.59	0.71	1.46	T	Arbour
2005bb	2839	II	0.41	-8.92	8.86	8.58	1.33	2.60	T	Lick Observa..
2005bn	8400	II	0.06	-10.08	9.05	8.78	0.84	2.43	I	SubbaRao, SD..
2005ci	2258	II	0.45	-9.78	8.72	8.57	0.70	1.71	T	Lick Observa..
2005dp	2676	II	1.29	-9.67	8.73	8.55	0.71	1.09	T	Itagaki
2005dq	6480	II	0.70					2.14	T	Armstrong
2005dz	5659	II	1.68					2.12	T	Puckett, Pel..
2005eb	4630	II	0.59					2.72	T	Lick Observa..
2005en	5210	II	0.64	-9.55	9.22	8.80	2.57	1.46	T	Puckett, Peo..
2005gi	15000	II	1.13					0.67	I	Sloan Digita..
2005gm	6643	II	1.94	-11.91			1.46	1.72	T	Lucas, Tron..
2005ip	2140	II	1.09	-9.10	9.13	8.86	0.70	2.06	T	Boles
2005kb	4590	II	0.72	-10.26	8.32	8.38	0.41	1.56	I	Sloan Digita..
2005kh	2220	II	111.00					1.72	T	LOSS
2005kk	5164	II	1.81					1.10	T	LOSS
2005lb	9000	II	0.71					2.18	I	Sloan Digita..
2005lc	3000	II	1.03	-9.70	8.32	8.37	0.02	1.57	I	Sloan Digita..
2005mg	3970	II	0.74					2.68	T	Newton, Puck..
2006J	5696	II	0.44					1.82	T	LOSS
2006O	5555	II	1.04					1.56	T	Rich
2006V	4752	II	2.03					2.38	T	Chen, Taiwan..
2006at	4500	II	0.85					2.65	T	Dintinjana, ..
2006be	2111	II	0.95	-9.75	8.83	8.54	0.73	2.10	T	LOSS
2006bj	11400	II	0.31	-10.23	8.79	8.64	0.69	2.07	I	Quimby
2006bx	5580	II	4.48					0.42	T	LOSS
2006by	5579	II	0.31	-10.53			2.87	2.77	T	LOSS
2006cx	5577	II	0.37					2.05	T	LOSS
2006dk	4941	II	0.89	-12.31			0.80	2.43	T	Migliardi
2006dp	5849	II	0.66					2.77	T	Monard
2006ed	5096	II	0.91	-9.74	9.01	8.75	1.91	1.74	T	LOSS
2006ee	4595	II	1.26					3.06	T	LOSS
2006ek	6088	II	4.26					2.51	T	LOSS
2006fg	9000	II	0.22					1.63	I	SDSS II coll..
2006gs	5710	II	0.84	-12.10			0.00	2.39	T	Itagaki
2006iu	6700	II	0.13					2.52	T	LOSS
2006iw	9000	II	0.87	-10.24	8.82	8.61	0.59	1.98	I	SDSS II coll..
2006kh	18000	II	0.52	-9.95	9.04	8.74	0.55	2.09	I	Sloan Digita..
2006pc	18000	II	1.13	-9.70	8.71	8.59	1.69	2.21	I	Sloan Digita..
2006qn	6496	II	0.39					2.06	T	Joubert, Li ..
2006st	3401	II	3.44					1.23	T	Winslow, Li ..
2007L	5456	II	1.82	-10.74			0.30	1.64	T	Mostardi, Li..
2007T	4033	II	1.28	-11.43			0.72	1.73	T	Madison, Li ..
2007am	3039	II	0.60	-9.63			0.99	1.64	T	Joubert, Li ..
2007an	3401	II	1.18	-8.29	8.99	8.69	1.19	1.24	T	Migliardi
2007be	3766	II	1.55	-10.33	9.05	8.79	1.80	2.73	T	Moretti, Tom..
2007fp	5646	II	0.36	-9.31	9.11	8.83	1.01	2.13	T	Liou, Chen, ..
2007gw	4941	II	0.72	-12.31			0.80	2.38	T	Itagaki
2007ib	9000	II	1.83	-10.02	9.01	8.76	0.67	0.93	I	Sloan Digita..
2007il	6349	II	1.08	-10.36	9.08	8.78	0.86	1.57	T	Chu, Li (LOS..
2007jn	18000	II	0.99					1.20	I	Sloan Digita..
2007kw	21000	II	1.83					1.43	I	Sloan Digita..
2007ky	21000	II	1.19					2.53	I	Sloan Digita..
2007lb	18000	II	154.72					0.60	I	Sloan Digita..
2007ld	9000	II	0.62					0.79	I	Sloan Digita..
2007lj	12000	II	0.61					1.53	I	Sloan Digita..
2007lx	17160	II	1.23	-9.16	8.70	8.45	0.11	1.55	I	Sloan Digita..
2007md	15000	II	1.10					2.71	I	Sloan Digita..
2007sz	6000	II	1.46					0.96	I	ESSENCE
2007tn	15000	II	1.34					2.17	I	ESSENCE
2008N	2382	II	0.41	-8.91	9.13	8.84	1.47	2.38	T	Winslow, Li,..
2008aa	6744	II	0.82					2.44	T	Madison, Li,..
2008ak	2377	II	0.78					1.79	T	Boles; Londe..
2008bh	4406	II	1.06					1.92	T	Pignata et a..
2008bj	5686	II	0.71	-9.93	8.37	8.38	0.05	1.23	I	Yuan et al. ..
2008bl	4417	II	0.81	-10.27	9.07	8.84	0.32	1.14	T	Duszanowicz
2008bx	2518	II	0.53					1.04	T	Puckett, Gag..
2008ch	4013	II	0.70					2.79	T	LOSS
2008dw	3786	II	0.45	-9.48	8.42	8.36	0.45	0.86	T	LOSS
2008ej	6331	II	0.36					3.73	T	LOSS
2008gd	17700	II	1.50	-10.28	8.84	8.66	0.89	1.33	I	Yuan et al. ..
2008gz	1857	II	0.51					2.02	T	Itagaki

TABLE 7 — *Continued*

SN	Vel. (km s ⁻¹)	Type	Offset Norm.	SSFR	T04 (dex)	PP04 (dex)	A _V (mag)	u'-z' (local)	Discov. Method	Discoverer
2009H	1414	II	0.96	-8.58	8.91	8.63	0.91	2.56	T	LOSS
2009af	2671	II	0.55					2.12	T	Cortini
2009at	1503	II	0.73	-10.33	8.97	8.73	1.87	2.68	T	Noguchi
2009ay	6650	II	0.94					2.19	T	Puckett, Peo..
2009bj	8100	II	0.39					2.79	I	"Palomar TF" ..
2009bk	11700	II	1.08	-10.19	8.70	8.60	0.28	0.80	I	"Palomar TF" ..
2009bl	12000	II	1.10	-10.39	8.78	8.63	0.56	1.27	I	"Palomar TF" ..
2009ct	18000	II	1.98					1.85	I	"Palomar Tra..
2009dd	723	II	0.19	-8.20	9.09	8.76	2.20	2.74	T	Cortini
2009fe	14100	II	0.73					2.42	I	Kasliwal et ..
2009hd	726	II	0.72	-9.54	9.15	8.84	0.94	1.81	T	Monard
2009jd	7546	II	2.39					1.09	I	Catelan, Dra..
2009jw	5856	II	0.35	-10.26	9.04	8.77	1.15	2.60	T	LOSS
2009ls	835	II	0.58	-10.98	8.96	8.77	0.26	1.93	T	Nishiyama, K..
2009nu	12000	II	1.82					0.47	I	Prieto, Drak..
2010K	6000	II	0.53					1.16	I	Prieto, Drak..
2010aw	6878	II	1.59	-8.20	8.62	8.29	0.63	1.36	T	LOSS
2010gq	5416	II	0.47	-10.10	9.13	8.84	1.04	2.59	I	Novoselnik e..
2010gs	8131	II	1.19	-10.69			1.39	2.15	I	Novoselnik e..
2010ib	5621	II	0.64					1.44	T	Cenko et al...
2010id	4956	II	7.52					0.00	T	Cenko et al...
1993G	3033	IIL	0.86	-9.38			2.26	2.05	T	Treffers, Le..
2006W	4757	IIL	1.07					2.70	T	LOSS
1990H	1580	IIP	0.45	-10.95			1.40	2.80	T	Perlmutter, ..
1991G	723	IIP	1.11	-7.71	8.99	8.51	1.18	2.28	T	Mueller
1998bv	1500	IIP	1.26	-9.26	8.11	8.18	0.04	1.14	T	Kniazev et a..
1998dl	1414	IIP	0.88	-8.58	8.91	8.63	0.91	2.10	T	Lick Observa..
1999ev	927	IIP	1.08					3.17	T	Boles
1999gi	588	IIP	0.65	-8.32	9.19	8.90	0.95	1.21	T	Kushida
1999gn	1574	IIP	0.86	-8.24	9.25	8.84	0.60	1.16	T	Dimai
1999gq	260	IIP	1.06	-9.81	7.86	8.21	0.43	1.03	T	Lick Observa..
2000db	681	IIP	0.76	-8.10	8.87	8.46	0.86	1.31	T	Aoki
2001R	4337	IIP	1.59					2.07	T	Lick & Tena..
2001X	1457	IIP	0.88	-9.15	9.15	8.84	0.93	2.15	T	Beijing Astr..
2001dc	2126	IIP	0.73	-11.69			2.06	2.69	T	Armstrong
2001dk	5400	IIP	1.29					2.09	T	Boles
2001fv	1469	IIP	1.47	-11.19			0.04	2.16	T	Armstrong
2001ij	11363	IIP	0.85		8.99	8.75	0.37	2.20	I	Sloan Digita..
2002ik	9600	IIP	1.56	-10.68			1.49	2.04	I	Sloan Digita..
2003J	775	IIP	0.57	-9.75	8.95	8.71	2.23	3.39	T	Puckett, New..
2003Z	1273	IIP	1.37	-10.43	9.06	8.74	1.20	1.85	T	Qiu, Hu
2003aq	5478	IIP	0.88	-9.57	8.95	8.70	0.52	1.60	T	Boles
2003gd	632	IIP	1.66					0.94	T	Evans
2003ie	697	IIP	1.22	-8.90	9.09	8.80	0.59	0.84	T	Arbour
2004A	853	IIP	1.90					2.03	T	Itagaki
2004am	300	IIP	0.22	-8.45			5.12	4.82	T	Lick Observa..
2004cm	1317	IIP	0.09	-9.19	8.73	8.48	3.81	1.96	I	SDSS
2004dd	4044	IIP	0.91					1.29	T	Lick Observa..
2004dg	1351	IIP	1.04				1.30	1.99	T	Vagnozzi et ..
2004dj	130	IIP	1.33	-11.03	8.52	8.55	0.00	3.21	T	Itagaki
2004du	5027	IIP	0.65					2.88	T	Lick Observa..
2004ez	1570	IIP	1.64	-8.04	9.07	8.69	0.87	1.84	T	Itagaki
2004fc	1807	IIP	0.16	-10.03	9.01	8.75	1.11	2.98	T	Lick Observa..
2005ad	1580	IIP	2.01	-8.84	8.91	8.58	0.27	1.25	T	Itagaki
2005ay	809	IIP	1.02	-8.88	9.10	8.74	0.81	1.34	T	Rich
2005cs	461	IIP	0.62	-10.17	9.05	8.78	0.24	1.11	T	Kloehr
2006bp	987	IIP	1.60					2.16	T	Itagaki
2006fq	21000	IIP	0.42	-9.68	8.99	8.69	0.67	1.66	I	SDSS II coll..
2006my	805	IIP	1.08	-9.53	9.05	8.82	1.19	2.35	T	Itagaki
2006ov	1574	IIP	0.85	-8.24	9.25	8.84	0.60	1.13	T	Itagaki
2007aa	1449	IIP	1.63	-8.83	9.23	8.87	0.79	1.38	T	Doi
2007aq	6292	IIP	3.25	-10.15	9.14	8.79	1.11	1.22	T	Winslow, Li ..
2007av	1422	IIP	0.20	-10.46	9.01	8.77	1.60	3.35	T	Arbour
2007bf	5309	IIP	1.60	-12.07			0.58	1.60	T	Puckett, Gui..
2007jf	21000	IIP	0.89	-10.05	8.42	8.43	0.35	1.95	I	Sloan Digita..
2007nw	18000	IIP	0.75					2.19	I	Sloan Digita..
2007od	1739	IIP	3.37					2.19	T	Maticic (PIK..
2008F	5406	IIP	1.93					3.07	T	Puckett, Sos..
2008X	1980	IIP	0.61	-10.31	8.59	8.57	0.37	1.39	T	Boles; Winsl..
2008az	2918	IIP	0.42					2.26	T	Newton, Gagl..
2008ea	4500	IIP	0.88					2.08	T	Martinelli, ..
2008hx	6596	IIP	0.80	-8.95	9.09	8.79	1.96	2.79	T	LOSS
2008in	1574	IIP	1.86	-7.60	8.91	8.37	0.84	2.24	T	Itagaki
2009A	5160	IIP	1.37					0.55	T	Pignata et a..
2009E	1980	IIP	1.34	-10.31	8.59	8.57	0.37	0.20	T	Boles

TABLE 7 — *Continued*

SN	Vel. (km s ⁻¹)	Type	Offset Norm.	SSFR	T04 (dex)	PP04 (dex)	A _V (mag)	u'-z' (local)	Discov. Method	Discoverer
2009W	5100	IIP	2.45					0.15	I	Drake et al...
2009am	3745	IIP	1.33	-9.92	9.09	8.82	1.76	2.95	T	LOSS
2009ao	3355	IIP	0.82	-10.03	9.15	8.78	1.94	2.39	T	Pignata et a..
2009bz	3253	IIP	1.09	-9.94	8.58	8.42	0.11	1.19	T	LOSS
2009dh	18000	IIP	1.34					2.29	I	Drake et al...
2009ga	3445	IIP	0.76					1.67	T	Itagaki
2009hf	3824	IIP	1.58					2.28	T	Monard
2009hq	2066	IIP	1.43	-8.45	8.84	8.50	0.68	1.39	T	Monard
2009ie	5328	IIP	2.54					1.07	T	LOSS
2009lx	8054	IIP	2.35	-10.68			1.61	1.81	I	Drake et al...
2009md	1302	IIP	0.85	-10.12	9.01	8.77	0.87	1.70	T	Itagaki
2009my	3311	IIP	1.06					1.17	T	LOSS
2010aj	6351	IIP	1.17					1.19	T	Newton, Puck..
2010fx	5122	IIP	1.60					1.55	T	Newton, Puck..
2010gf	5555	IIP	1.01					1.56	T	Cenko et al...
2010hm	6121	IIP	1.48					2.62	T	Cenko et al...
2010jc	7248	IIP	2.29	-11.95			0.00	0.56	I	Howerton et ..
1999br	1021	IIP pec	1.21	-8.43	9.03	8.65	0.53	1.95	T	Lick Observa..
2000em	5700	II pec	0.43					2.60	T	Nearby Galax..
2001dj	5251	II pec	3.41					2.90	T	Lick & Tena..
2003cv	8400	II pec	0.92					1.17	I	NEAT/Wood-Va..
2004by	3532	II pec	1.51					1.14	T	Armstrong
2004gg	6017	II pec	1.40					2.26	T	Lick Observa..
2007ms	12000	II pec	0.25					0.94	I	Sloan Digita..
2006G	5031	II/IIb	1.23					2.94	T	LOSS
PTF09dxv	9900	IIb	1.29					3.29	I	PTF
PTF09fae	20100	IIb	0.86					0.65	I	PTF
1996cb	711	IIb	1.19	-9.68	8.54	8.39	0.47	0.96	T	Aoki
1997dd	4554	IIb	2.21	-8.34	9.23	8.69	1.24	0.63	T	Aoki
2001ad	3315	IIb	2.01	-10.52	8.81	8.70	0.26	0.00	T	Beijing Astr..
2001gd	877	IIb	1.78	-9.47	8.87	8.59	0.76	1.23	T	Itagaki; Dim..
2003ed	1348	IIb	0.51	-8.60	8.93	8.55	1.07	1.31	T	Itagaki
2004ex	5217	IIb	1.85					1.82	T	Trondal, Sch..
2004gj	6182	IIb	1.29	-9.41	8.99	8.69	0.91	1.73	T	Lick Observa..
2005U	3088	IIb	0.27	-9.38			2.26	0.98	T	Mattila et a..
2005la	5570	IIb	1.25					1.23	I	Quimby, Mond..
2006dl	6556	IIb	1.03	-9.80	9.05	8.79	1.02	1.90	T	LOSS
2006iv	2407	IIb	3.10	-10.19	8.53	8.43	0.08	1.67	T	Duszanowicz
2006qp	3748	IIb	1.47	-11.48			0.84	2.00	T	Itagaki
2006ss	3591	IIb	1.21	-10.23	8.96	8.73	0.35	0.79	T	Boles
2007ay	4359	IIb	0.99					1.32	T	Mostardi, Li..
2007rw	2568	IIb	0.99	-9.39	8.69	8.47	0.18	0.87	T	Madison, Li ..
2008ax	579	IIb	1.07	-8.38	8.71	8.21	0.55	1.78	T	Mostardi, Li..
2008cw	9724	IIb	0.14	-9.51	8.32	8.34	0.24	1.21	I	Yuan et al. ..
2008cx	5649	IIb	1.64	-10.94			0.85	0.60	T	Monard
2008ie	4107	IIb	1.24					2.94	T	Pignata et a..
2009K	3497	IIb	0.36					3.05	T	Pignata et a..
2009ar	7800	IIb	0.22					1.31	I	Mahabal, Dra..
2009fi	4770	IIb	0.91	-9.82	8.66	8.52	0.45	1.09	T	Boles
2009jv	4826	IIb	0.39	-9.63	9.00	8.76	2.31	1.61	T	Gorelli, New..
2010am	6000	IIb	1.80					0.77	I	Drake et al...
1994Y	2554	IIIn	0.67	-8.28	9.13	8.79	0.74	2.52	T	Wren
1995G	4873	IIIn	1.37					1.42	T	Evans, Shobb..
1996ae	1563	IIIn	0.93	-10.64			3.05	3.36	T	Vagnozzi, Pi..
1996bu	1158	IIIn	2.19					2.34	T	Kushida
1997ab	3750	IIIn	0.86	-9.87	8.40	8.36	0.15	1.53	T	Hagen, Reime..
1998S	838	IIIn	0.93	-9.77	9.09	8.82	1.63	2.38	T	BAO Supernov..
1999eb	5412	IIIn	0.57					1.79	T	Lick Observa..
1999gb	5153	IIIn	0.93	-9.03	9.12	8.84	0.90	1.38	T	Lick Observa..
2000ev	4388	IIIn	0.92					1.34	T	Manzini
2001I	4963	IIIn	0.78					2.11	T	Lick & Tena..
2001fa	5241	IIIn	0.67					2.07	T	Lick & Tena..
2002ea	4342	IIIn	0.62	-10.15	9.15	8.78	1.43	2.53	T	Puckett, New..
2002fj	4406	IIIn	0.71					2.03	T	Monard
2003G	3449	IIIn	0.53					2.74	T	LOTOSS
2003dv	2271	IIIn	2.53					1.11	T	LOTOSS
2003ke	6176	IIIn	0.83	-9.88	9.08	8.75	2.02	2.26	T	Lick Observa..
2004F	5248	IIIn	0.56	-8.80	8.99	8.69	0.84	2.07	T	Lick Observa..
2005cp	6630	IIIn	0.51					1.81	T	Lick Observa..
2005db	4495	IIIn	0.88					2.47	T	Monard
2005gl	4682	IIIn	0.96					1.66	T	Puckett, Cer..
2006aa	6198	IIIn	0.89	-9.63	9.22	8.83	1.55	1.90	T	LOSS
2006am	2676	IIIn	0.95	-9.67	8.73	8.55	0.71	1.55	T	LOSS
2006bo	4602	IIIn	1.28					1.73	T	Boles
2006cy	10800	IIIn	1.78					1.16	I	Quimby, Mond..

TABLE 7 — *Continued*

SN	Vel. (km s ⁻¹)	Type	Offset Norm.	SSFR	T04 (dex)	PP04 (dex)	A _V (mag)	u'-z' (local)	Discov. Method	Discoverer
2006db	6900	IIn	1.17	-10.27	8.33	8.40	0.14	0.98	I	Quimby, Mond..
2006gy	5631	IIn	0.17					3.26	I	Quimby
2006jd	5563	IIn	1.42					0.72	T	LOSS
2006tf	22200	IIn	0.43					0.86	I	Quimby, Cast..
2007K	6505	IIn	0.88	-12.47			0.00	2.82	T	Madison, Li ..
2007cm	4937	IIn	1.43	-11.58			0.75	2.14	T	Kloehr
2007rt	6700	IIn	0.28	-10.31	9.05	8.72	1.17	2.05	T	Li (LOSS)
2008B	5715	IIn	0.86	-9.76	9.14	8.83	1.29	1.46	T	Itagaki
2008fm	11557	IIn	1.77					1.78	I	Yuan et al. ..
2008gm	3475	IIn	1.42					1.33	T	Pignata et a..
2008ip	4538	IIn	2.15	-11.92			0.94	2.73	T	Kobayashi
2008ja	20700	IIn	0.56					1.57	I	Catelan, Dra..
2009nn	13800	IIn	1.29					1.59	I	Zheng, Yuan ..
2010jl	3300	IIn	0.51	-7.89	8.12	8.15	0.62	0.26	T	Newton, Puck..
1994W	1226	IInP	0.96	-10.34			1.99	2.18	T	Cortini, Vil..
2007pk	5011	IIn pec	0.63					1.26	T	Parisky, Li ..
2010al	5116	IIn pec	0.69	-10.80	8.95	8.69	1.07	2.01	T	Rich
PTF09awk	18600	Ib	0.10	-9.32	8.61	8.39	0.28	1.51	I	PTF
PTF09dfk	4800	Ib	0.65					1.32	I	PTF
1991ar	4562	Ib	0.79					1.39	T	McNaught, Ru..
1997dc	3445	Ib	0.49					2.20	T	BAO Supernov..
1998T	3033	Ib	0.23	-9.38			2.26	0.96	T	BAO Supernov..
1998cc	4337	Ib	1.16					2.34	T	Lick Observa..
1999di	4921	Ib	1.01					1.68	T	Puckett, Lan..
1999dn	2808	Ib	6.24					1.80	T	Beijing Obse..
1999eh	1955	Ib	0.75	-9.66	8.99	8.74	2.35	1.77	T	Armstrong
2000de	2400	Ib	0.64	-9.69	8.88	8.62	0.35	1.20	T	Migliardi
2000dv	4098	Ib	0.73					2.01	T	Lick Observa..
2000fn	4669	Ib	0.95	-10.00	8.92	8.75	1.03	2.03	T	Holmes
2002dg	14000	Ib	1.23					0.86	I	NEAT/Wood-Va..
2002hz	5414	Ib	0.59					2.72	T	LOTOSS
2003I	5329	Ib	1.16	-10.17	9.01	8.74	1.14	1.70	T	Puckett, Lan..
2003bp	5934	Ib	0.91	-9.46	8.99	8.74	1.31	1.64	T	LOTOSS
2003gk	3218	Ib	1.11					1.19	T	LOTOSS
2004ao	1690	Ib	0.52					1.40	T	Lick Observa..
2004bs	5164	Ib	0.45	-9.65	8.98	8.72	0.79	2.05	T	Armstrong
2004gv	5995	Ib						1.83	T	Chen
2005O	5646	Ib	0.57	-9.31	9.11	8.83	1.01	2.73	T	Chen
2005bf	5704	Ib	1.31					2.44	T	Monard; Lick..
2005hl	6000	Ib	1.71	-9.85	9.16	8.83	1.54	1.78	I	Sloan Digita..
2005hm	9000	Ib	0.26					1.77	I	Sloan Digita..
2005mn	15000	Ib	0.22	-9.86	8.71	8.53	0.52	1.91	I	Sloan Digita..
2006ep	4495	Ib	2.20					2.37	T	LOSS; Itagaki..
2007ag	6211	Ib	0.52	-9.69	8.98	8.72	1.96	2.56	T	Puckett, Gag..
2007ke	5202	Ib	0.69					3.22	T	Chu, Li (LOS..
2007qx	18000	Ib	0.58					2.05	I	Sloan Digita..
2007uy	1955	Ib	0.56	-9.66	8.99	8.74	2.35	1.79	T	Hirose
2008D	1955	Ib	1.00	-9.66	8.99	8.74	2.35	1.79	T	Swift/XRT sa..
2008ht	6486	Ib	1.21	-11.04			0.38	1.74	T	LOSS
2009ha	4411	Ib	0.87					1.63	T	Monard
2009jf	2379	Ib	1.50					0.74	T	LOSS
2010O	3033	Ib	0.35	-9.38			2.26	1.89	T	Newton, Puck..
2002hy	3806	Ib pec	0.83					1.95	T	Monard
2006jc	1671	Ib pec	1.36	-10.49	8.49	8.53	0.13	1.64	T	Itagaki; Puc..
2009lw	4914	Ib/IIb	1.57					1.56	T	LOSS
2010P	3033	Ib/IIb	1.02	-9.72			1.54	2.15	T	Mattila, Kan..
2002dz	5349	Ib/c	0.88					2.05	T	LOTOSS
2003A	6548	Ib/c	0.70					2.18	T	LOTOSS
2003ih	4963	Ib/c	1.39					2.01	T	Armstrong
2006lc	4906	Ib/c	0.98	-11.34			1.82	2.69	I	Sloan Digita..
2006lv	2477	Ib/c	0.86	-9.42	8.58	8.52	0.60	1.76	T	Duszanowicz
2007kj	5260	Ib/c	1.83					2.79	T	Itagaki
2007sj	12000	Ib/c	0.52	-10.41	9.10	8.76	1.04	2.40	I	Sloan Digita..
2008fn	8940	Ib/c	0.65					3.00	I	Yuan et al. ..
2008fs	11580	Ib/c	0.77					2.26	I	Yuan et al. ..
2010br	697	Ib/c	0.28	-8.90	9.09	8.80	0.59	2.88	T	Nevski
2010gr	5131	Ib/c	1.33					2.27	T	Cenko et al...
2010is	6275	Ib/c	0.73					2.25	T	Cenko et al...
2001co	5166	Ib/c pec	1.06	-10.80			2.82	2.46	T	Lick & Tena..
PTF10bhu	10800	Ic	0.71	-10.32	8.61	8.53	0.46	1.94	I	PTF
PTF10bip	15300	Ic	0.68					1.39	I	PTF
2005az	2572	Ic	0.72	-10.61	8.81	8.71	0.66	1.77	I	Quimby et al.
1990B	2255	Ic	0.42	-9.77	9.23	8.76	3.23	3.11	T	Perlmutter, ..
1990U	2379	Ic	1.06					1.84	T	Pennypacker,..
1991N	989	Ic	0.74					0.53	T	Perlmutter, ..

TABLE 7 — *Continued*

SN	Vel. (km s ⁻¹)	Type	Offset Norm.	SSFR	T04 (dex)	PP04 (dex)	A _V (mag)	u'-z' (local)	Discov. Method	Discoverer
1994I	461	Ic	0.34	-8.32	9.15	8.86	1.33	2.10	T	Puckett, Arm..
1995F	1514	Ic	0.24	-10.50	9.07	8.84	0.73	2.54	T	Lane, Gray
1995bb	1740	Ic	0.37					1.91	T	Tokarz, Garn..
1996D	4723	Ic	0.59					2.31	T	Drissen, Rob..
1996aq	1602	Ic	0.52	-9.89	9.01	8.74	0.64	1.27	T	Aoki
1997X	1108	Ic	0.48	-9.28	9.07	8.79	0.67	1.86	T	Aoki
1997ei	3204	Ic	0.43	-9.34	9.14	8.83	0.93	2.16	T	Aoki
1999bc	6299	Ic	0.85	-9.71	9.16	8.76	1.46	1.49	I	Supernova Co..
1999bu	2722	Ic	0.28	-8.71	9.09	8.76	1.22	3.20	T	Lick Observa..
2000C	3810	Ic	1.40					1.36	T	Foulkes; Mig..
2000cr	3505	Ic	1.08	-11.73			0.55	2.09	T	Migliardi, D..
2000ew	958	Ic	0.47	-11.17			1.87	1.78	T	Puckett, Lan..
2001ch	2931	Ic	0.49					0.45	T	Lick & Tena..
2001ci	1101	Ic	0.27					3.11	T	Lick & Tena..
2002J	3806	Ic	0.72					2.38	T	LOTOSS
2002ao	1552	Ic	0.95	-9.93	8.55	8.41	0.24	0.94	T	LOTOSS
2002hn	5153	Ic	0.27	-9.03	9.12	8.84	0.90	1.70	T	LOTOSS
2002ho	2527	Ic	0.87					1.96	T	Boles
2002jj	4218	Ic	0.35					2.88	T	LOTOSS
2003L	6373	Ic	0.67	-8.47	9.11	8.74	1.30	1.60	T	Boles; LOTOS..
2003el	5671	Ic	0.94	-9.18	9.25	8.88	2.06	2.80	T	LOTOSS
2003hp	6220	Ic	1.68					1.30	T	LOTOSS
2004C	1656	Ic	0.95	-9.49	9.01	8.74	1.94	2.75	T	Dudley, Fisc..
2004aw	4742	Ic	2.07	-8.23	8.95	8.56	1.08	1.86	T	Boles; Itaga..
2004bf	5130	Ic	0.71	-8.81	8.94	8.56	1.81	1.49	T	Lick Observa..
2004bm	1153	Ic	0.05	-9.30	9.27	8.91	1.61	2.83	T	Lick Observa..
2004cc	2255	Ic	0.24	-9.77	9.23	8.76	3.23	3.25	T	Lick Observa..
2004dc	6306	Ic	0.54					2.89	T	Lick Observa..
2004fe	5316	Ic	1.01					1.63	T	Lick Observa..
2004gn	1732	Ic	0.70	-9.41	9.11	8.84	3.68	2.67	T	Lick Observa..
2005aj	2547	Ic	1.27					1.92	T	Puckett, New..
2005eo	5210	Ic	1.19	-9.55	9.22	8.80	2.57	2.23	T	Puckett, Peo..
2005kl	988	Ic	0.50	-8.86	9.09	8.77	1.39	1.40	T	Migliardi
2006dg	4274	Ic	0.95					2.00	T	LOSS
2006fo	6000	Ic	0.73	-9.06	9.07	8.74	0.90	2.14	I	SDSS II coll..
2007ce	13800	Ic	0.90					0.00	I	Quimby
2007cl	6650	Ic	0.59					1.64	T	Puckett, Sos..
2007nm	13800	Ic	0.63					2.38	I	Djorgovski e..
2007rz	3806	Ic	0.89					1.80	T	Parisky, Li ..
2008ao	4473	Ic	1.47					1.21	T	Migliardi, L..
2008du	4820	Ic	0.92					1.36	T	LOSS
2008ew	6080	Ic	0.83	-9.34	8.97	8.74	0.56	2.43	T	LOSS
2008fo	9000	Ic	1.30	-9.52	8.83	8.61	0.90	1.67	I	Yuan et al. ..
2008hh	5768	Ic	1.14					1.69	T	Puckett, Cro..
2008hn	3358	Ic	0.87	-9.88	9.06	8.82	0.89	1.93	T	LOSS
2009em	1730	Ic	0.81					1.89	T	Monard
2009lj	4465	Ic	1.77					1.91	T	LOSS
2010Q	16500	Ic	0.56					0.76	I	Graham, Drak..
2010do	4295	Ic	1.11	-8.98	9.26	8.89	2.07	1.25	T	Monard; Cen..
2010gk	4293	Ic	0.30	-9.19	9.13	8.79	2.84	2.62	T	Li, Cenko et..
2010io	1991	Ic	0.32					0.61	T	Duszanowicz
2003id	2344	Ic pec	1.07					1.79	T	LOTOSS
PTF09sk	10650	Ic-bl	0.77	-9.34	8.36	8.30	0.71	1.23	I	PTF
1997dq	958	Ic-bl	1.59	-8.23	9.00	8.48	0.85	1.43	T	Aoki
1997ef	3539	Ic-bl	1.23	-9.36	9.13	8.86	1.54	1.22	T	Sano
1998ey	4806	Ic-bl	1.15					2.72	T	Arbour
2002ap	632	Ic-bl	2.69					0.00	T	Hirose
2002bl	4757	Ic-bl	0.94	-9.70	9.12	8.76	2.53	2.19	T	Armstrong
2003jd	5635	Ic-bl	0.57					0.96	T	Lick Observa..
2004bu	5549	Ic-bl	0.43	-9.89	8.70	8.47	0.92	2.82	T	Boles
2004ib	16800	Ic-bl	0.56	-10.05	8.48	8.48	0.65	2.20	I	Frieman, SDS..
2005nb	7128	Ic-bl	0.58	-8.39	8.57	8.33	0.53	0.85	I	Quimby et al.
2006aj	9900	Ic-bl	0.77					3.28	I	Cusumano et ..
2006nx	15000	Ic-bl	1.22					0.87	I	Sloan Digita..
2006qk	18000	Ic-bl	0.19					3.28	I	Sloan Digita..
2007I	6487	Ic-bl	0.76	-9.53	8.36	8.37	0.88	1.32	T	Lee, Li (LOS..
2007bg	10200	Ic-bl	3.58					0.97	I	Quimby, Ryko..
2010ah	14940	Ic-bl	0.93					1.34	I	Ofek et al. ..
2010ay	20100	Ic-bl	0.16	-8.70	8.58	8.21	0.29	0.97	I	Drake et al...

NOTE. — The Off. Norm. column is the deprojected offset of the SN explosion site normalized by the host g' -band half-light radius. Method column denotes whether we designated the survey that discovered the SN as targeted (T) or galaxy-impartial (I). The Discoverer column is taken from the IAU catalog^a.

^a <http://www.cfa.harvard.edu/iau/lists/Supernovae.html>